B 7 Galvanomagnetic Transport: from Hall Effect to AMR

P. S. Bechthold
Institut für Festkörperforschung
Forschungszentrum Jülich GmbH
e-mail: p.bechthold@fz-juelich.de

Contents

Lecture notes presented at the 40th IFF Spring School ,
Forschungszentrum Jülich, 9th – 20th March 2009,
see: http://hdl.handle.net/2128/3592

1 Introduction

Galvanomagnetic transport denotes the transport properties of metals and semiconductors under the simultaneous action of electric and magnetic fields. If we apply an electric field $\mathbf{E}$ to a homogeneous metal or semiconductor it will generate a current that on a wide range of conditions will obey Ohm's law , which on a microscopic level states a linear relationship between the local current density $\mathbf{j}$ and the field $\mathbf{E}$:

$$\mathbf{j} = \sigma \mathbf{E}. \tag{1}$$

σ is the electrical conductivity. Equivalently, we could have written

$$\mathbf{E} = \rho \mathbf{j}. \tag{2}$$

where ρ is the resistivity, the inverse of the conductivity. More general, a charged particle moving in an electromagnetic field is subject to the Lorentz force

$$\mathbf{F} = q(\mathbf{E} + \mathbf{v} \times \mathbf{B}), \tag{3}$$

where q is the charge of the particle, $\mathbf{E}$ is an accelerating electric field, $\mathbf{v}$ is the velocity of the particle and $\mathbf{B}$ is the magnetic flux density or magnetic induction. Thus, a free electron moving with a constant velocity $\mathbf{v}$ (electric field $\mathbf{E} = \mathbf{0}$) perpendicular to a homogeneous field $\mathbf{B}$ will be forced into a circular motion according to

$$\frac{mv^2}{r} = |e|vB. \tag{4}$$

Here $|e|$ is the modulus of the electron charge, r is the radius of the trajectory and mv^2/r is the modulus of the centripetal force. The time of circulation is $T = 2\pi r/v$ which defines the cyclotron frequency

$$\omega_c = \frac{2\pi}{T} = \frac{eB}{m}, \tag{5}$$

which for nonrelativistic particles does not depend on the particle velocity and the radius of the trajectory. This equation remains valid for conduction electrons in solids, as well, if we replace the free-electron mass m by the cyclotron mass m_c. [1]

Now, if we apply an electric field and perpendicular to it a magnetic field to a conducting solid the vector of the current density will no longer be parallel to the electric field, at least for a short time (see above). In general, the presence of a magnetic field will generate an anisotropy so that the current-density vector will deviate from the direction of the applied electric field. We then have to define a tensorial relationship between the current density and the applied fields which for the vector components - referred to a right handed orthonormal reference system (x, y, z) gives:

$$j_i = \sigma^0_{ij} E_j + \alpha_{ijk} E_j B_k + \beta_{ijkl} E_j B_k B_l + higher\ order\ terms \quad (i, j, k, l = x, y, z). \tag{6}$$

[1] In case of spherical energy surfaces (Fermi surfaces) the cyclotron mass is identical to the effective mass. In more general cases it can be calculated from the effective mass tensor [1]:

$$m^*_{ij}(\mathbf{k}) = [\frac{1}{\hbar^2} \frac{\partial^2 \epsilon(\mathbf{k})}{\partial k_i \partial k_j}]^{-1}.$$

Here we have used Einstein's summation convention which says that the sum has to be taken over repeated indices on the right hand side of the equation. The extra index 0 at σ_{ij}^0 will become clear below. The tensor components $\sigma_{ij}^0, \alpha_{ijk}$ and β_{ijkl} are material constants and are subject to symmetry restrictions which depend on the crystallographic symmetry of the sample material [2]. This looks quite complicated, but if there are no second order or higher order terms in the electric field components we can – as is usually done – include all the magnetic field contributions into a generalized definition of the electric conductivity. The price, we have to pay, is that now the conductivity tensor will depend on the magnetic field.

$$j_i = \sigma_{ij}(\mathbf{B})E_j. \tag{7}$$

With these conditions the σ_{ij}^0 components in eq. 6 correspond to $\sigma_{ij}(\mathbf{B} = \mathbf{0})$. Using the Onsager relations [3] we get the symmetry restriction

$$\sigma_{ij}(\mathbf{B}) = \sigma_{j\,i}(-\mathbf{B}). \tag{8}$$

That is, the conductivity tensor is symmetric with respect to a simultaneous reversal of the magnetic induction. For the reverse relation (2) we now get:

$$E_j = \rho_{j\,i}(\mathbf{B})j_i, \tag{9}$$

where $\underline{\underline{\rho}}$ is the inverse tensor of $\underline{\underline{\sigma}}$.
The components of both these tensors are related by

$$\rho_{ii} = (\sigma_{jj}\sigma_{kk} - \sigma_{jk}\sigma_{kj})/\Delta(\sigma);\ \rho_{ij} = (\sigma_{ik}\sigma_{kj} - \sigma_{ij}\sigma_{kk})/\Delta(\sigma) \tag{10}$$

where $\Delta(\sigma)$ is the determinant of σ_{ij}.
Similarly,

$$\sigma_{ii} = (\rho_{jj}\rho_{kk} - \rho_{jk}\rho_{kj})/\Delta(\rho);\ \sigma_{ij} = (\rho_{ik}\rho_{kj} - \rho_{ij}\rho_{kk})/\Delta(\rho). \tag{11}$$

In the absence of a magnetic field, σ_{ij} and $\rho_{\,ij}$ are symmetrical, $\sigma_{ij} = \sigma_{j\,i}$, and this implies that a sytem of orthogonal axes can be found, with respect to which they are diagonal. When a field $\mathbf{B}$ is present the tensors are generally not symmetrical and each of them requires all nine components for a complete specification.
In the following we will only consider constant currents, i.e. DC currents. Moreover, we will assume that our sample is at a constant temperature. We will ignore the Joule heating and therefore exclude any temperature gradients. We will also restrict the discussion to the low-field limit throughout this contribution. In mathematical terms this situation is described by $\omega_c\tau \ll 1$ where τ is the scattering time of the charge carriers. This means that the charge carriers are scattered many times by phonons, impurities or defects before they can complete a full cyclotron orbit. In this case we do not need to worry about Landau level quantization or any quantum oscillations that occur in the high field limit $\omega_c\tau \gg 1$, and may lead, for example, to the quantum Hall effect.
The remainder of this contribution is organized as follows. In Chapter 2 we will start with a phenomenological description of the galvanomagnetic transport based on the classical equations of motion. In the subsequent chapters we will deal with the galvanomagnetic behaviour of non-magnetic materials and first discuss the ordinary Hall effect and then the Lorentz magnetoresistance. In this course we will soon realize that the classical description is insufficient and that a quantum mechanical model based on the Pauli principle (Fermi statistics) and electronic

band structure – the so called semiclassical model – will be needed to understand and interpret the experimental observations. Within this framework we will then derive an equation for the electrical conductivity with the aid of the Boltzmann equation. Finally, we will study what changes when the materials are ferromagnetic themselves and carry an internal magnetization. We will finish this contribution with a basic description of the anisotropic magnetoresistance (AMR) and its applications.

2 Phenomenology of Galvanomagnetic Transport

The first attempt to calculate the electrical conductivity was made by Drude prior to the development of the quantum theory [1, 4].
His model is based on the assumption of a free electron gas moving in the confinement of a metal block, interacting with the metal ions only through elastic collisions. Today we know that Drudes model is only valid within certain limits as we shall also see below. But much of his Ansatz remains applicable when certain quantities like velocities, the carrier masses and the results are interpreted in terms of band structure theory [2].
Drude's starting point was the classical equation of motion:

$$m\frac{dv}{dt} + \gamma v = -e\ E, \tag{12}$$

where he introduced a velocity dependent damping ($\gamma = m/\tau$) due to scattering processes. v is the drift velocity of the electrons which decays with a relaxation time τ when the accelerating field is switched off. The superimposed thermal motion of the carriers averages to zero. In the stationary state we have $dv/dt = 0$ and we get

$$v = -\frac{e\tau}{m}\ E = -\mu E. \tag{13}$$

Thus the drift velocity is proportional to the accelerating field where the quantity

$$\mu = \frac{e\tau}{m} \tag{14}$$

is called the charge carrier mobility. With a charge carrier density n we then get a current density

$$j = -env = en\mu E. \tag{15}$$

Together with Ohm's law

$$\mathbf{j} = \sigma \mathbf{E}. \tag{16}$$

we finally get the conductivity

$$\sigma = en\frac{e\tau}{m} = en\mu. \tag{17}$$

The conductivity is proportional to the charge, the density, and the mobility of the charge carriers. It increases with the relaxation time which is a measure of the time between scattering events.

[2] Sommerfeld extended his model to a quantum mechanical free electron gas by introducing the Pauli principle through the Fermi-Dirac distribution function. This was later further extended by introducing the lattice periodicity caused by a weak periodic potential and leading to the band structure model with Bloch functions, reciprocal lattices, Brillouin zones etc [1].

Now we extend equation (12) by introducing an additional magnetic field:

$$m\frac{d\mathbf{v}}{dt} + \frac{m}{\tau}\mathbf{v} = -e\ (\mathbf{E} + \mathbf{v} \times \mathbf{B}), \tag{18}$$

In the stationary state $d\mathbf{v}/dt = 0$ we then get

$$\mathbf{v} = -\frac{e\tau}{m}\ (\mathbf{E} + \mathbf{v} \times \mathbf{B}) = -\mu(\mathbf{E} + \mathbf{v} \times \mathbf{B}). \tag{19}$$

The current density now becomes:

$$\mathbf{j} = -en\mathbf{v} = en\mu\mathbf{E} - \mu(\mathbf{j} \times \mathbf{B}) = \sigma_0\mathbf{E} - \mu(\mathbf{j} \times \mathbf{B}) \tag{20}$$

where $\sigma_0 = \sigma(B = 0)$. Without loss of generality we may assume that $\mathbf{B}$ is aligned with the z-direction of our coordinate sytem. Then we can write equation (20) in terms of components:

$$\begin{aligned} j_x &= \sigma_0 E_x - \mu B_z j_y \\ j_y &= \sigma_0 E_y + \mu B_z j_x \\ j_z &= \sigma_0 E_z \end{aligned} \tag{21}$$

or since $\mu B_z = \tau\frac{e}{m}B_z = \tau\omega_c$

$$\begin{aligned} \sigma_0 E_x &= j_x - \tau\omega_c j_y \\ \sigma_0 E_y &= \tau\omega_c j_x + j_y \\ \sigma_0 E_z &= j_z \end{aligned} \tag{22}$$

or in matrix notation ($\rho_0 = 1/\sigma_0$):

$$\begin{pmatrix} E_x \\ E_y \\ E_z \end{pmatrix} = \rho_0 \begin{pmatrix} 1 & (\tau\omega_c) & 0 \\ -(\tau\omega_c) & 1 & 0 \\ 0 & 0 & 1 \end{pmatrix} \begin{pmatrix} j_x \\ j_y \\ j_z \end{pmatrix} = \rho_{ij}(B_z) j_j \tag{23}$$

or

$$\begin{pmatrix} E_x \\ E_y \\ E_z \end{pmatrix} = \rho_0 \begin{pmatrix} 1 & (\mu B_z) & 0 \\ -(\mu B_z) & 1 & 0 \\ 0 & 0 & 1 \end{pmatrix} \begin{pmatrix} j_x \\ j_y \\ j_z \end{pmatrix} = \rho_{ij}(B_z) j_j \tag{24}$$

and

$$\begin{pmatrix} j_x \\ j_y \\ j_z \end{pmatrix} = \frac{\sigma_0}{1 + (\tau\omega_c)^2} \begin{pmatrix} 1 & -(\tau\omega_c) & 0 \\ (\tau\omega_c) & 1 & 0 \\ 0 & 0 & 1 + (\tau\omega_c)^2 \end{pmatrix} \begin{pmatrix} E_x \\ E_y \\ E_z \end{pmatrix} = \sigma_{ij}(B_z) E_j \tag{25}$$

or

$$\begin{pmatrix} j_x \\ j_y \\ j_z \end{pmatrix} = \frac{\sigma_0}{1 + (\mu B_z)^2} \begin{pmatrix} 1 & -(\mu B_z) & 0 \\ (\mu B_z) & 1 & 0 \\ 0 & 0 & 1 + (\mu B_z)^2 \end{pmatrix} \begin{pmatrix} E_x \\ E_y \\ E_z \end{pmatrix} = \sigma_{ij}(B_z) E_j. \tag{26}$$

We see now that the presence of a magnetic field renders the resistivity and the conductivity anisotropic quantities even for an isotropic material. The conductivities and resistivities have changed in the (x, y)-plane. The consequences of this will be discussed in the next chapters.

3 Hall Effect

This effect was discovered by Edwin H. Hall during his PhD-work and was published in 1879 [5, 6, 7]. Let us assume a non-magnetic slab of a conducting material with parallel planes, length l, width b and thickness d like the one depicted in Fig. 1 and a coordinate system as indicated in the figure. We apply an electric field parallel to the long axis and a magnetic field perpendicular to the slab. When we switch on the electric field the charge carriers will initially be deflected sideways by the Lorentz force, the charges will get accumulated at one side, until the generated electric forces completely balance the Lorentz force. At steady state conditions the current will flow parallel to the applied electric field and we can measure a "Hall"-voltage U_H between the sample sides. The stationary-state condition is that the Lorentz force and the transverse electric force cancel each other, i.e.:

$$F_y = -e(\mathbf{v} \times \mathbf{B})_y - eE_y = ev_xB_z - eE_y = 0, \tag{27}$$

where v_x is the drift velocity of the charges and $E_y = U_H/b$ is the Hall field. When we assume that only electrons are the charge carriers – like in metals or n-doped semiconductors at suffiently low temperatures – the current density in the x-direction is $j_x = -en_ev_x = i/(b \cdot d)$. Here, n_e is the electron density of the sample and i is the total current. Therefore we get

$$U_H = E_y \cdot b = -\frac{1}{n_e e} j_x B \cdot b = -\frac{1}{n_e e} i\ B/d = R_H i\ B/d. \tag{28}$$

R_H is called Hall coefficient. Thus, by measuring the current i, the field $\mathbf{B}$, the thickness d of the slab and the Hall voltage U_H we can determine the charge carrier density n_e of our sample. What we have obtained here is the standard textbook derivation of the Hall field [8]. We could have obtained this result also from our equations (23) - (26) by putting the transverse current $j_y = 0$. We will now use this relation to calculate the current density in our sample. With $j_y = 0$ from equation (26) we get $(\mu B_z)E_x + E_y = 0$. Thus the longitudinal current density gets:

$$j_x = \frac{\sigma_0}{1 + (\mu B_z)^2}(E_x - (\mu B_z)E_y) = \frac{\sigma_0}{1 + (\mu B_z)^2}(E_x + (\mu B_z)^2 E_x) = \sigma_0 E_x. \tag{29}$$

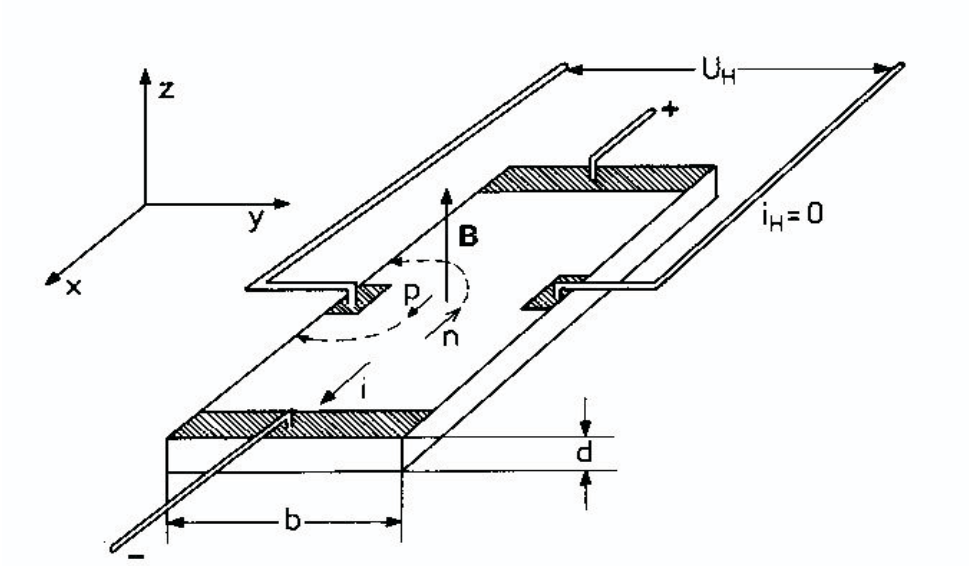

Fig. 1: *Scheme of a Hall arrangement [8].*

Despite the anisotropy in equation (26) the resistivity of the longitudinal current has not changed. Experimentally, however, one might observe changes in the resistance. One simple reason is in the velocity distribution of the charge carriers [9, 10]. This means that the Lorentz force is slightly different for different charge carriers, while the action of the Hall field is always the same. Accordingly, the Lorentz forces are compensated on average only. Individual charges might still be slightly deflected from their ideal trajectories. The longer path lengths then lead to an increase of the resistivity. Anyway, to measure significant changes in the resistance – the so called magnetoresistance – we have to prevent the formation of the Hall field. How this can be done will be discussed in the next section.

To get a significant Hall signal the sample should be thin and the charge-carrier density should not be too large. That is why semiconductors are the preferred materials in Hall sensors.

In p-doped semiconductors the Lorentz force on holes is directed toward the same side of the sample, because of their positive charge and opposite drift velocity. Thus, if we consider a p-doped semiconductor at low temperature, where mainly holes are the charge carriers, the electric field E_y and with it the polarity of the voltage U_H and the Hall coefficient will change sign. Therefore, from the sign of the voltage and the Hall coefficient we will be able to distinguish the charge type of the main carriers.

While monovalent metals – particularly the alkalis – nicely obey this simple classical rule others strongly deviate. The deviations observed in ferromagnetic metals will be addressed below. Some divalent group IIA and group IIB metals even show a reversed sign of the Hall coefficient [3]. The reason is found in their electronic structure, which has to be treated quantum mechanically. The atoms of the group II metals all exhibit a fully occupied s^2 electronic subshell. Thus, one might rather expect a weak van der Waals like bond rather than a metallic bond. Dimers and small clusters of these materials are indeed very weakly bound. They become metallic in character at larger particle sizes, because the s-subshell finally hybridizes with the respective p-subshell. Thus, at the Fermi level one expects an almost completely filled valence band with a negative curvature resulting in a negative effective electron mass. This contribution can be replaced by the compensating contribution of holes – now with positive effective mass.

A more rigorous treatment of positive charge carriers in metals can be obtained from a detailed investigation of the Fermi surface. We want to illustrate this with the aid of Fig. 2. It shows schematically the Harrison construction of a fictitious square reciprocal lattice with Fermi spheres that exceed the first Brillouin zone. The rule that Fermi surfaces should cut the zone boundary at right angles is ignored here for clarity. According to the Pauli principle only a small fraction of electrons in the Fermi sphere can contribute to the charge transport. They are located in an energy range of the order of kT around the Fermi energy. In a semiclassical approach we may consider an electron as a wave packet moving in reciprocal space [1, 12]. Its velocity in k-space is the group velocity of this wave packet:

$$\mathbf{v}(k) = \frac{\partial \omega}{\partial \mathbf{k}} = \frac{1}{\hbar}\frac{\partial \varepsilon(\mathbf{k})}{\partial \mathbf{k}} = \frac{1}{\hbar}\nabla_{\mathbf{k}}\varepsilon(\mathbf{k}) \tag{30}$$

Its momentum is $\mathbf{p} = \hbar\mathbf{k}$. The equation of motion of the electron in a magnetic field is then

$$\hbar\frac{d\mathbf{k}}{dt} = -e(\mathbf{v}(\mathbf{k}) \times \mathbf{B}). \tag{31}$$

From these equations we learn that the electron moves perpendicular to $\mathbf{B}$ and $\mathbf{v}(\mathbf{k})$ in k-space. Moreover, $\mathbf{v}(\mathbf{k})$ points in the direction of a gradient of a constant energy surface which is the

[3] In this situation, the simple Drude model fails.

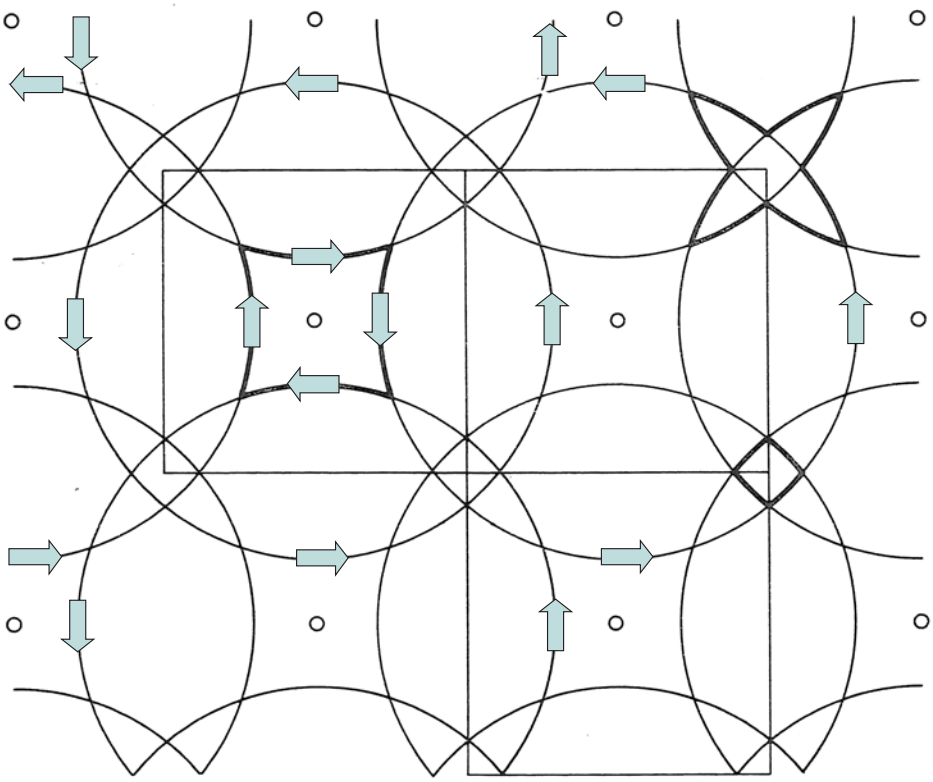

Fig. 2: *Simplified scheme of a reciprocal lattice with Fermi spheres that exceed the size of the first Brillouin zone. A square hole pocket is formed that can contribute a positive part to the Hall coefficient of a metal or semiconductor. See text for details. [11].*

direction perpendicular to the surface. In other words: in k-space the electron moves tangential to a constant energy surface which is the Fermi surface or in the simplified picture of fig. 2 the Fermi sphere. Let us assume that all the electrons move counterclockwise around the Fermi surface as indicated by the arrows in the figure. Then we see that at the surface of the accentuated square the electrons move clockwise around the square. This is precisely the behaviour of positive charges which make a positive contribution to the Hall coefficient. Thus, the square is a hole pocket. This picture is also consistent with the imagination of an almost completely filled band, because if we fill up the Fermi spheres with more electrons the Fermi spheres will expand and the hole pocket will shrink. When the spheres completely overlap the hole pocket will disappear. The respective band is then filled up and will no longer contribute to the charge transport. This simple example shows that the Fermi surfaces of materials need to be studied very carefully if Hall coefficients are to be determined.

From this simple consideration we must conclude that the charge transport in the quantum mechanical treatment deviates drastically from the classical picture. In the classical picture the current is equally carried by all the electrons. In the quantum mechanical picture only a small fraction of the electrons in the vicinity of the Fermi level will contribute to the conductivity, all moving approximately with the Fermi velocity. The rest is blocked by the Pauli principle. The classical picture assumes that the electrons collide with ion cores. In quantum mechanics, if the ion cores are kept in their perfect lattice positions there will be no scattering at all. This is because the electrons are described by Bloch waves. They are eigenfunctions of the system and therefore they are time independent. Thus, quantum mechanically scattering can occur only

due to lattice imperfections, i. e. phonons, impurities and defects, including surfaces. In the quantum picture the conduction phenomena occur close to the Fermi surface, and despite the defects mainly the differences of the Fermi surfaces are determining the conduction behavior of the materials.
Why then can we use classical formulas at all? This point will be addressed in chapter 5 on the Boltzmann equation, which takes into account the Fermi-Dirac distribution and leads to the same conductivity formula as the classical picture. With this in mind we have to check all the results deduced from the classical approach for their consistency with quantum mechanics. It is an interesting aspect of this consideration that the classical formulas could only be saved by introducing positive charge carriers into quantum mechanics.
With these remarks we come back to the Hall effect. When both type of charge carriers contribute to the Hall effect the equation for the Hall coefficient must be modified. In general the signal will contain contributions from both electrons and holes and the sign of the Hall coefficient determines whether electrons or holes are the dominant charge carriers. This is particularly the case for semiconductors at elevated temperatures, where (due to intrinsic conduction) electrons and holes simultaneously contribute to the charge carriers. In the presence of both charge carriers we then have to deal with an ambipolar current and the valence and conduction band simultaneously. In this case not only the carrier densities (n_e for electrons and n_h for holes), but also the drift mobilities (μ_e and μ_h) of the carriers become involved. In general, the charge carriers will have different mobilities in both bands, usually $\mu_h < \mu_e$. With highly doped samples at sufficiently low temperatures essentially only one type of charge carriers will contribute to the conduction. In such cases one can get back to the single-band picture discussed above. The following equation allows us to calculate the Hall voltage. Its somewhat lengthy derivation is given in the appendix.

$$U_H = E_H \cdot b = \frac{n_h\mu_h^2 - n_e\mu_e^2}{e(n_h\mu_h + n_e\mu_e)^2} j_x B_z \cdot b = \frac{n_h - n_e(\mu_e/\mu_h)^2}{e(n_h + n_e\mu_e/\mu_h)^2}\, iB/d. \tag{32}$$

Here the ratio of the mobilities has been introduced. If electrons and holes had the same density and the same mobility, they would completely compensate each other. In reality this is not the case. The Hall field will change sign depending whether there are more electrons or more holes accumulated by the Lorentz force. U_H changes sign at $n_h = n_e(\mu_e/\mu_h)^2$ rather than at the intrinsic concentration $n_h = n_e$. This equation is widely used to characterize Hall coefficients of semiconductors and metals.
With these results we can now interpret the temperature behaviour of the Hall coefficient of InSb as given in Fig. 3 [13, 9, 14, 15] . InSb is a low band gap semiconductor $\varepsilon_g = 0.18eV$ and an important sensor material. The figure shows the modulus of the Hall coefficient as a function of the inverse temperature for various degrees of doping (temperature from right to left given in the upper legend). The letters A and B refer to n-doped samples, the numbers 1 to 4 to p-doped samples with increasing concentration of the dopend in this order. The sample denoted by V is the purest. The concentration of the dopant varies from $10^{13}/cm^3$ (curve V) to $2 \times 10^{17}/cm^3$ (curve 4) [13, 15]. As can be seen at low temperatures the modulus of the Hall coefficient decreases with increasing doping due to the increasing carrier density. For a given doping level it is largely constant at low temperatures, because of the fixed carrier concentration supplied by the dopant. This is true also for the sample V, which seems to have a small concentration of free electrons due to some remaining impurities. When the temperature increases the growing number of electron-hole pairs finally leads to an exponential decrease of the Hall coefficient as drastically demonstrated for the pure sample. Since electrons exhibit

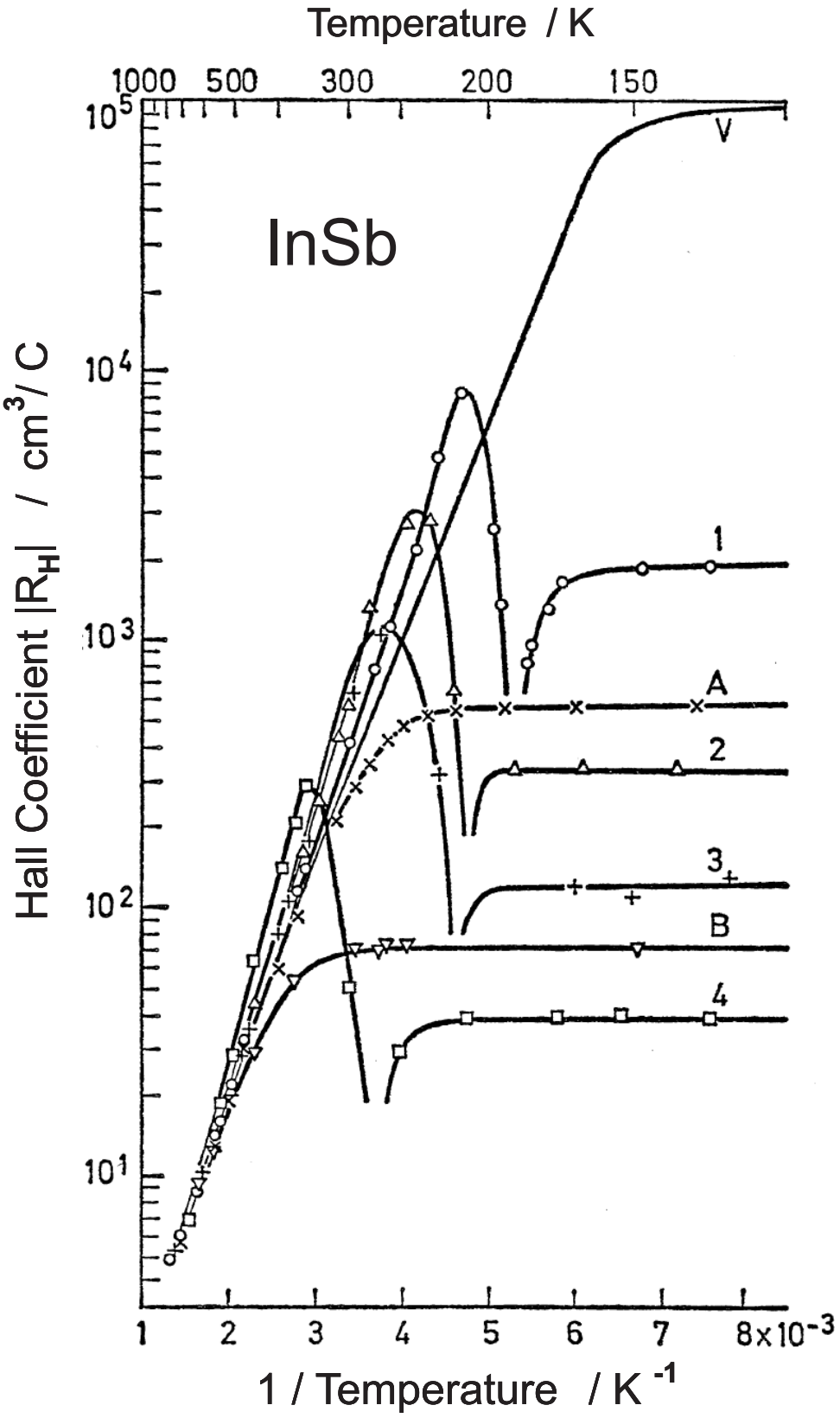

Fig. 3: *Modulus of the Hall coefficient of InSb at various degrees of doping as a function of the inverse temperature. [9, 13, 14, 15].*

a larger mobility the n-doped samples – as well as the pure sample – have a negative Hall coefficient and gradually approach the line of intrinsic conduction (curves V, A and B). In contrast, the initially positive Hall coefficient of the p-doped samples changes sign when the density of intrinsic carriers reaches a certain level. Then, it even slightly overshoots the intrinsic conduction line and finally approaches it from the other side. Naturally, the crossing of the zero line occurs at lower temperatures for samples with initially lower p-dopend concentration.
So far, we have treated all carriers alike except for the sign. In reality, they may have an energy distribution, anisotropic masses and different relaxation times. In such cases, it might be necessary to include correction factors to the simple equations given above. These factors are usually of the order of one [15, 16].
From the sign of the Hall coefficient we learn whether electrons or holes are the primary charge carriers. For a single band from the measurement of the Hall coefficient we can determine the density and the charge sign of the carriers. From the equation

$$\mu = R_h \sigma$$

and a simultaneous determination of the conductivity, we can also identify the carrier mobility. Van der Pauw [17] has described procedures to avoid and minimize experimental errors in Hall measurements. Today the Hall effect is widely used to either measure magnetic fields with calibrated Hall sensors or to determine carrier densities and mobilities of carriers in semiconductors.

4 Lorentz-Magnetoresistance

Just like the ordinary Hall effect, the Lorentz magnetoresistance (also called ordinary magnetoresistance (OMR)) occurs in all conducting materials. It describes the change of the material's resistivity when an external magnetic field is applied.
Depending on the direction of the magnetic field with respect to the current flow we distinguish between longitudinal and transverse magnetoresistance. The transverse effect is the more important. From our equations (23) - (26) we can see that the conductivity and the resistivity may change in the (x, y)-plane when a magnetic field is applied in the z-direction perpendicular to the film. To realize this situation we have to make use of the transverse current generated by the Lorentz force. In the Hall measurements we have eliminated the transverse current (on the average, see above) by building up an opposing electric field. As a result the resistivity of the thin film did not change with the magnetic field applied, at least in our simplified approach. Now we want to make use of the transverse current itself. To do so we have to avoid or to shortcut the opposing electric field. Suppose we have shortened the Hall field in Fig. 1 and apply an electric field in the x-direction $E_x = E_0$ and $E_y, E_z = 0$, we get from eqs. (23), (24): $E_x = \rho_0(j_x + (\mu B_z)j_y$. In addition, we have $E_y = -(\mu B_z)j_x + j_y = 0$ or $j_y = (\mu B_z)j_x$. For the electric field component in x-direction E_x this gives

$$E_x = \rho_0(1 + (\mu B_z)^2)j_x. \tag{33}$$

The resistance grows quadratically with the applied field. The relative increase of the resistance is usually measured by :

$$\frac{\rho(B) - \rho_0}{\rho_0} = \frac{\Delta\rho}{\rho_0} = (\mu B_z)^2 \tag{34}$$

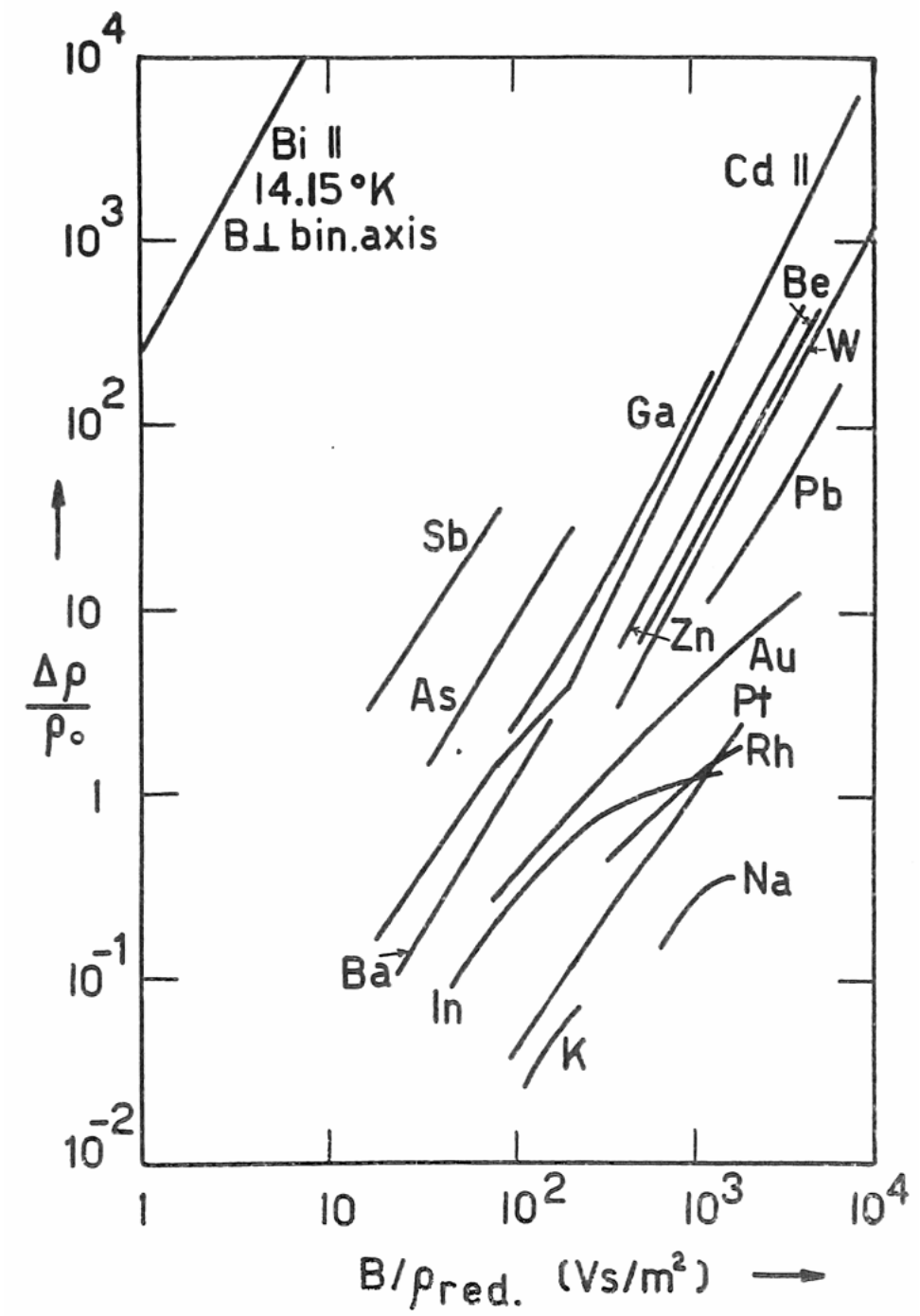

Fig. 4: *Reduced Kohler diagram where $\rho_{red} = \rho(T)/\rho(\Theta)$ and Θ is the Debye temperature of the metal. [20].*

It is this quantity that is usually called the "Lorentz magnetoresistance" or "ordinary magnetoresistance" (OMR) . The effect is qualitatively easy to understand. In between two subsequent scattering events the Lorentz force deflects the electrons on their way to the counterelectrode. This increases the electron path way and therefore the average number of collisions with phonons, impurities and defects. This consequently increases the resistance.

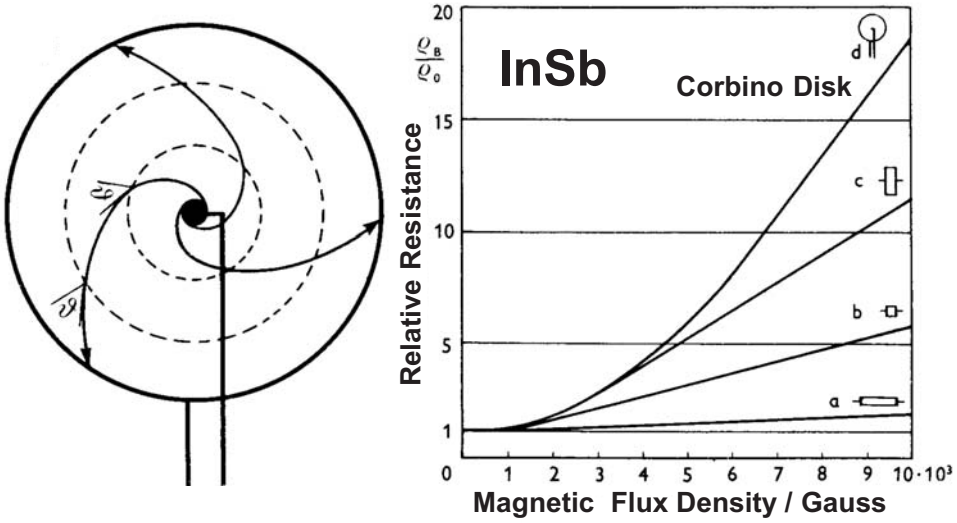

Fig. 5: *Left: Principle scheme of a Corbino disk. Right: Relative resistance as a function of magnetic induction for samples of n-doped InSb of equal purity, but different geometrical shape. The upper curve is that of a Corbino disk. Lower curves are for plain samples with differing length/width ratios (l/w =1/3, 1/1 and 10/1 from above). This demonstrates the influence of the geometrical factor. [9, 10].*

In simple metals in the low field limit it follows the scaling law

$$\frac{\rho(B) - \rho_0}{\rho_0} = \frac{\Delta\rho}{\rho_0} = const(B/\rho_0)^2, \tag{35}$$

i.e., for a given metal all measurements should follow the same parabola when $\Delta\rho/\rho_0$ is plotted versus B/ρ_0, independent of temperature or purity of the sample. This is known as Kohler's rule [4] [11, 19, 20, 21] . In our free electron approach this is evident, because $\mu B \propto \tau B$ and the scattering time is inversely proportional to ρ_0 for a given metal. Kohler's derivation is more rigorous, however, because it relies on the Boltzmann equation and thus includes the Pauli exclusion principle. Fig. 4 demonstrates that a variety of elementary metals nicely follows this rule. The Kohler rule is valid only, when all the participating charge carriers exhibit the same scattering time τ, i.e. the same microscopic scattering mechanisms. Deviations from Kohler's rule therefore indicate, that different scattering mechanisms might be at play in a sample.
In normal metals the Lorentz magnetoresistance is a small effect and has no technological applications. The only exception is the semimetal Bi, which exhibits $\sim 18\%$ magnetoresistance in a transverse field of 0.6 T [22]. Therefore, in early applications of the magnetoresistive effect a Bi-spiral was used to measure magnetic fields [23]. Later it was found that InSb shows an even larger Lorentz magnetoresistance [10], and this, indeed, led to technological applications (see below) .
Experimentally, the most effective way to avoid the formation of a Hall field is to use a Corbino disk (Fig. 5) [10, 18] . It consists of two concentric circular electrodes with the metallic or semi-

[4]The rule can even be extended to higher field ranges, when the quadratic field dependence is replaced by a material dependent function f:

$$\frac{\Delta\rho}{\rho_0} = f(B/\rho_0) \tag{36}$$

where, of course, f is parabolic in the low field limit.

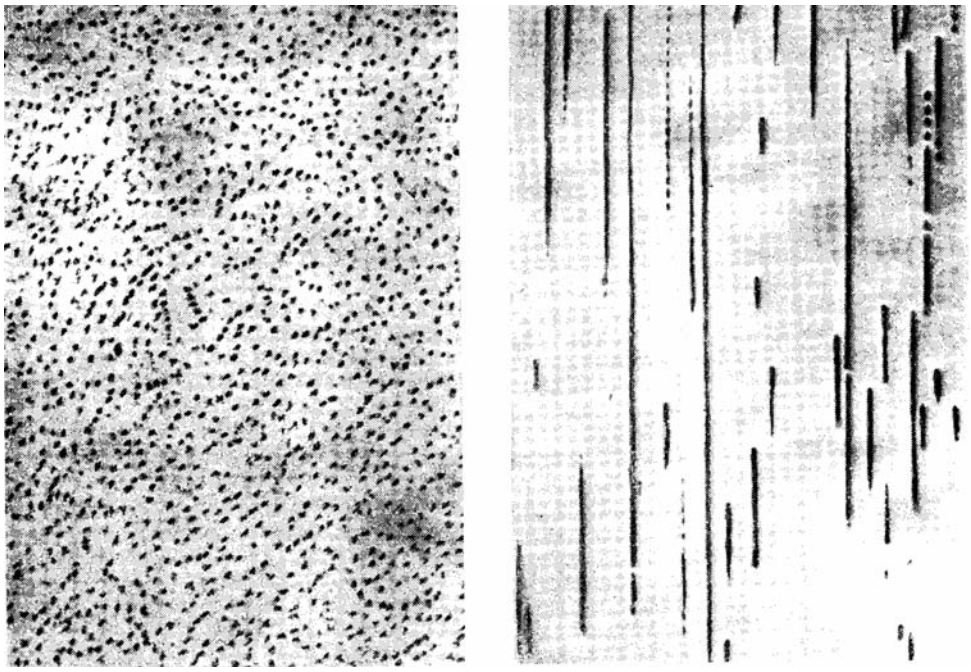

Fig. 6: *Micrographs of polished sections of an oriented InSb-NiSb eutectic as used in commercial Lorentz magnetoresistors. The samples were cut perpendicular and parallel, respectively, to the NiSb needles. The needles have diameters of about* $1\mu m$*. The length is up to about* $50\mu m$*. When oriented perpendicular to the applied electric field, the needles will shortcut the Hall field. Inside the needles the current will flow parallel to the needle axis, outside the needles it gets deflected by the Lorentz force [14, 24, 25].*

conducting material, e.g. InSb, in between. The externally applied electric field is then pointing in a radial direction and the equipotential lines are concentric circles, as well. Therefore, a balancing transverse Hall field cannot build up in this geometry. The trajectory of the current flow is a logarithmic spiral. The current meets every equipotential line at the same angle. The angle ϑ is defined by the ratio of the transverse to radial current density: $tan\vartheta = j_t/j_r$ and is called the Hall angle. With an applied magnetic field the resistance grows due to the magnetic field induced lengthening of the trajectories. Fig. 5 also shows the quadratic field dependence of the relative magnetoresistance of InSb for the Corbino disk and three other InSb samples of identical purity, but different length/widths ratio (1:3, 1:1 and 1:10). This demonstrates that the resistivity also depends on sample geometry [9, 10]. The latter effect will not be further dicussed here.

The Corbino Disk, while occasionally used in scientific studies is not suited for sensor applications, because it does not provide a large enough resistance to be useful for sensor applications. For larger resistances one has to elongate the current path length. This can be easily achieved by meandering a narrow stripe of material but then one has to meet precautions to avoid the occurance of the Hall field. The elegant solution to this is the "Feldplatte" also known as MDR (Magnetic field Dependent Resistor) . It was invented in the 1960's and since 1965 is available as a commercial product. It contains a meandering thin layer ($8-25\mu$m) of InSb which is doped with 1.8 % NiSb . At this concentration InSb and NiSb form an eutectic in which small needles of NiSb (Ø1μm, length up to 50μm) grow inside the InSb. At favourable growth conditions these needles orient parallel to the crystallographic growth front (e.g. in a Zone melting pro-

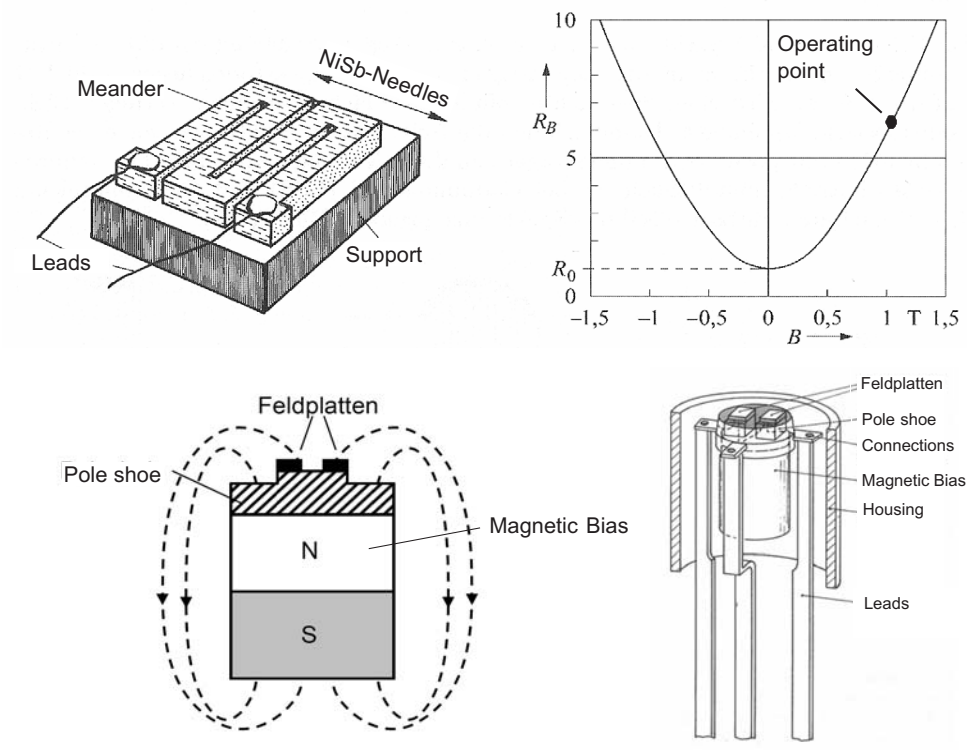

Fig. 7: *Upper left: Scheme of a meandering magnetoresistor based on the InSb-NiSb eutectic with the NiSb needles oriented perpendicular to the direction of the applied electric field. Upper right: the response curve of such a device. Lower left: Principle of magnetic bias for two "Feldplatten" combined in a bridge circuit. Lower right: Arrangement of two "Feldplatten" in a commercial device. [14, 24, 25, 26].*

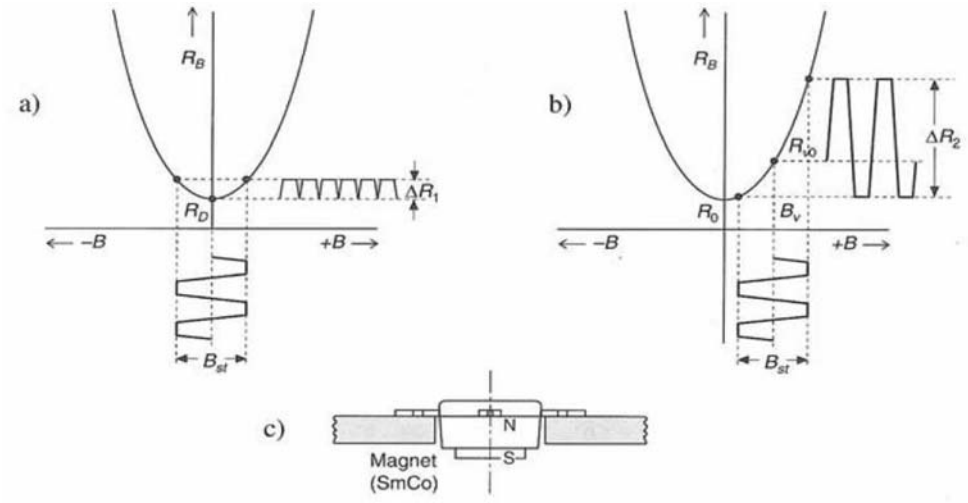

Fig. 8: *(a) Response of an unbiased Lorentz magnetoresistor. Positive and negative field directions cannot be distinguished. (b) Response of a magnetically biased magnetoresistor with the operating point shifted to the right in the figure. Now the field direction can be identified. Simultaneously the sensitivity is increased. (c) Mounting of a biased "Feldplatte" [25, 26].*

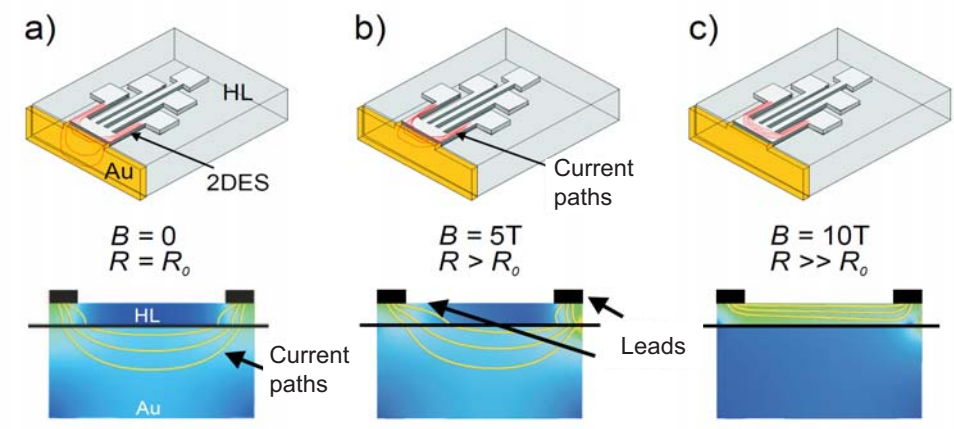

Fig. 9: *Simulation of the EMR-effect. At $B = 0$ the current passes preferentially through the gold contacts. With increasing magnetic field the current is more and more forced into the semiconducting layer (HL). This leads to an increase of the magnetoresistance [28].*

cess)(fig. 6) [14, 24, 25]. The conductivity of the NiSb is larger than that of InSb by two orders of magnitude. When oriented perpendicular to the applied electric field the needles, therefore, shorten the Hall field (fig. 7). Due to the meandering the resistance may be changed from a few Ω to some $k\Omega$. One obstacle of the "Feldplatte" is its temperature sensitivity. Commercial devices, therefore contain two of these resistors in a bridge circuit (figs. 7). One as a reference for temperature compensation. Because of the B^2 dependence of the resistivity, the "Feldplatte" cannot initially distinguish the direction of an applied magnetic field. Therefore, commercial devices are biased by a permanent hard magnetic layer (figs. 7 and 8). Then the field direction can be identified. It also increases the sensitivity due to the slope of the B^2 parabola and allows an adjustment of the operating point to the field strength desired. "Feldplatten" have been widely used as automotive sensors and even in space vehicles, but are currently more and more replaced by other magnetoresistive sensors. One reason is found in the difficulties to embed them into integrated circuits.

Nevertheless, InSb has recently regained new interest, since it was realized that it is possible to achieve drastic increases of the magnetoresistance simply by choosing favourable geometric arrangements of the resistor material and the metallic electrodes [27, 28, 29]. The arrangement is such that at $B = 0$ the current flows preferentially through the metallic leads. An increasing magnetic field more and more forces the current to flow through the semiconductor thereby increasing the resistance of the device. An example of a computer simulation of such an arrangement is shown in fig. 9 [28]. This effect is now called extraordinary magnetoresistance (EMR) . It is believed to possess great technological potential for future applications.

5 The Boltzmann Equation

With the aid of the Boltzmann equation we will now sketch how to derive an equation for the conductivity of our system. In chapter 2 we have discussed the charge carrier motion in terms of the classical Drude model. We have already seen that this is not in complete agreement with experimental findings. We will therefore discuss the transport properties in a more realistic band structure approach.
In the band picture the electrons are considered as independent particles moving in a weak perfectly periodic potential. Quantum mechanical solutions to this single particle model are the Bloch wave functions which have completely incorporated the interaction with the lattice potential. In the strictly periodic potential where the ion cores of the metal occupy their ideal periodic positions the Bloch electrons are not scattered because the Bloch waves are the eigenfunctions of the system. Thus scattering processes can occur only at deviations from the strict lattice periodicity, i.e. at lattice phonons, impurities, defects like dislocations, and at surfaces. Phonons are the dominant scatterers at higher temperatures, whereas defects and impurities become important at low temperatures where the lattice vibrations are frozen out. In a solid at thermal equilibrium the single particle energy levels are occupied according to the Fermi- Dirac distribution function.

$$f(E) = \frac{1}{1 + exp[(E - E_F)/k_B T]}. \tag{37}$$

Therefore, most of the electrons cannot contribute to interaction processes because they are hindered by the Pauly principle. Only those electrons with energies close enough to the Fermi level can take part.
In the so called semiclassical approach an electron is described by a wave packet in k-space consisting of a superposition of Bloch wave functions centered at a certain wave vector $\mathbf{k}$. The drift velocity of the electron is then given by the group velocity of this wave packet [1].

$$\mathbf{v}(k) = \frac{1}{\hbar}\nabla_k \varepsilon_{\mathbf{k}} = \frac{1}{\hbar}\frac{\partial \varepsilon(\mathbf{k})}{\partial \mathbf{k}} \tag{38}$$

$\mathbf{v}(\mathbf{k})$ is parallel to the gradient of the surface of constant energy in k-space, i.e. it is not in general parallel to the wave vector. The electron wave packet is extended in r- and in k-space. The Δr and Δk values thereby have to obey the uncertainty relation $\Delta r \Delta k \approx 1$. The spread of the wavepacket is assumed to be small with respect to the dimensions of the Brillouin zone. Then in the direct lattice its extension is large compared to the dimensions of the unit cell. For completely free electrons the energy band is a parabola in k-space $\varepsilon(\mathbf{k}) = \frac{\hbar^2 k^2}{2m}$ and we get $\mathbf{v}(\mathbf{k}) = \frac{\hbar \mathbf{k}}{m}$.
If we consider $\hbar\mathbf{k}$ as the momentum of the electron in k-space the equation of motion with an applied Lorentz force is:

$$\frac{d\mathbf{k}}{dt} = -\frac{e}{\hbar}(\mathbf{E} + \mathbf{v} \times \mathbf{B}). \tag{39}$$

An external electric field will accelerate the electrons and therefore change the energy distribution. The small distortions due to phonons or due to impurities scatter the electrons with the tendency to restore equilibrium.
We will now describe the effect of the externally applied fields and the scattering processes on the distribution function of the electrons and seek the variation of the distribution function with time. For simplicity we will assume that only one single band is involved.

We consider a volume in phase space and consider the flow of particles in and out. The change in the distribution function is:

$$df/dt = \partial f/\partial t + (\partial f/\partial \mathbf{r})(\partial \mathbf{r}/\partial t) + (\partial f/\partial \mathbf{k})(\partial \mathbf{k}/\partial t) = (\partial f/\partial t)_{coll} \tag{40}$$

where the last term is the change of the function due to collisions. We can rewrite this equation in the form:

$$df/dt = \partial f/\partial t + \dot{\mathbf{k}} \cdot \nabla_k f + \dot{\mathbf{r}} \cdot \nabla_r f = \frac{\partial f}{\partial t}|_{coll}. \tag{41}$$

This is the Boltzmann equation. It is the starting point for the discussion of the transport phenomena. Introducing the above values for $\mathbf{v_k}$ and $d\mathbf{k}/dt$ gives

$$\partial f/\partial t + \mathbf{v}(\mathbf{k})(\partial f/\partial \mathbf{r}) - (e/\hbar)(\mathbf{E} + \mathbf{v} \times \mathbf{B})(\partial f/\partial \mathbf{k}) = (\partial f/\partial t)_{coll} \tag{42}$$

Since we have assumed that there are no thermal gradients in our system we get $\partial f/\partial \mathbf{r} = 0$. To proceed further we have to specify the collision term. This is quite complicated in general [30, 31]. Here we will use the relaxation time approximation . Thereby it is assumed that the deviation of the distribution function from the equilibrium distribution function f_0 (the Fermi-Dirac function) is small:

$$f(\mathbf{k}) = f_0(\mathbf{k}) + f_1(\mathbf{k}). \tag{43}$$

Further it is assumed that the collision term can be expressed as

$$(\partial f/\partial t)_{coll} = -\frac{f(\mathbf{k}) - f_0(\mathbf{k})}{\tau} = -\frac{f_1(\mathbf{k})}{\tau}. \tag{44}$$

where τ is the relaxation time. It determines the rate of return to the equilibrium distribution when the external field is switched off because then we have

$$(\partial f/\partial t) = -\frac{f(\mathbf{k}) - f_0(\mathbf{k})}{\tau}. \tag{45}$$

The general solution to this is

$$f(t) = f_0 + [f(0) - f_0]e^{-t/\tau} \tag{46}$$

where $f(0)$ is the distribution at the time when the fields are switched off. Thus the non-equilibrium distribution decays exponentially towards the equilibrium distribution when the driving fields are switched off. Introducing the collision term (44) into the Boltzmann equation (42) we get

$$\partial f/\partial t - (e/\hbar)(\mathbf{E} + \mathbf{v} \times \mathbf{B})(\partial f/\partial \mathbf{k}) = -\frac{f(\mathbf{k}) - f_0(\mathbf{k})}{\tau} \tag{47}$$

Since we are interested in a stationary state we have $\partial f/\partial t = 0$. We will here also omit the influence of the magnetic field.[5] We are the then left with:

$$-(e/\hbar)\mathbf{E}(\partial f/\partial \mathbf{k}) = -\frac{f(\mathbf{k}) - f_0(\mathbf{k})}{\tau} \tag{48}$$

which can be rewritten as

$$f(\mathbf{k}) = f_0(\mathbf{k}) + (e/\hbar)\tau\mathbf{E}(\partial f/\partial \mathbf{k}) \tag{49}$$

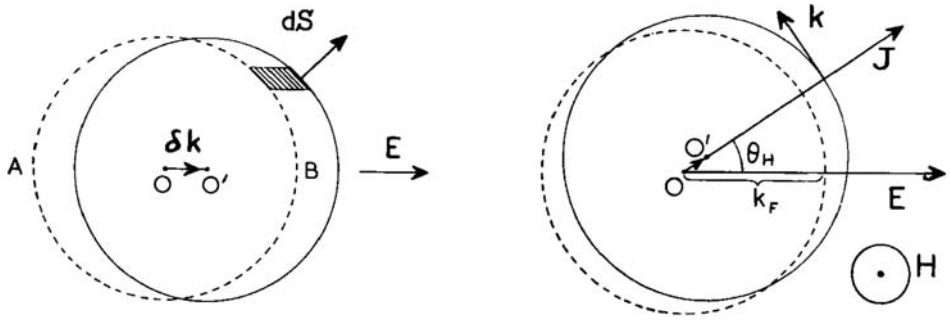

Fig. 10: *Displacement of the Fermi sphere, (a) by an electric field, (b) by an electric field and a magnetic field normal to the page [12].*

This equation can be solved iteratively by replacing $\partial f/\partial \mathbf{k}$ by $\partial f_0/\partial \mathbf{k}$ in the first step [8]

$$f(\mathbf{k}) \approx f_0(\mathbf{k}) + (e/\hbar)\tau \mathbf{E}(\partial f_0/\partial \mathbf{k}). \tag{50}$$

The right side may be considered as the first elements of a Taylor series of a function

$$f(\mathbf{k}) = f_0(\mathbf{k} + (e/\hbar)\tau \mathbf{E}). \tag{51}$$

Therefore the effect of a weak electric field in k-space is simply a shift of the Fermi sphere by an amount $\delta k = (e/\hbar)\tau E$ in the direction of the electric field (Fig. 10(a)). A magnetic field applied in addition will rotate the displaced Fermi sphere by the Hall angle about the direction of the magnetic field (Fig. 10(b)) [12].
The carrier density is given by integration over k-space

$$n = \frac{2}{8\pi^3} \int f(\mathbf{k}) d\mathbf{k}. \tag{52}$$

The factor 2 is due to the two spin directions spin $\uparrow$ and spin $\downarrow$, the factor $1/(2\pi)^3$ due to the k-space integration [32]. With that the current density gets:

$$\mathbf{j} = -\frac{e}{4\pi^3} \int \mathbf{v}(\mathbf{k}) f(\mathbf{k}) d\mathbf{k}. \tag{53}$$

This can be written

$$\mathbf{j} = -\frac{e}{4\pi^3} \left(\int \mathbf{v}(k) f_0(\mathbf{k}) d\mathbf{k} + \int \mathbf{v}(\mathbf{k}) f_1(\mathbf{k}) d\mathbf{k} \right) \tag{54}$$

where the first term $\int \mathbf{v}(\mathbf{k}) f_0(\mathbf{k}) d\mathbf{k} = 0$ because of the antisymmetric integrand. At zero applied electric field there is no net current flow. Introducing the above value for

$$f_1 = (e/\hbar)\tau \mathbf{E}(\partial f_0/\partial \mathbf{k}) = (e/\hbar)\tau \mathbf{E}(\partial f_0/\partial \varepsilon)(\partial \varepsilon/\partial \mathbf{k}) = e\tau \mathbf{E}\mathbf{v}(\mathbf{k})(\partial f_0/\partial \varepsilon) \tag{55}$$

gives

$$\mathbf{j} = -\frac{e^2 \mathbf{E}}{4\pi^3} \int \tau \mathbf{v}(\mathbf{k}) \mathbf{v}(\mathbf{k}) (\partial f_0/\partial \varepsilon) d\mathbf{k}. \tag{56}$$

[5] a more general treatment including the magnetic field is given in the literature [9, 11, 12, 15, 30, 31]

For the conductivity tensor this results in

$$\underline{\underline{\sigma}} = \frac{e^2}{4\pi^3} \int \tau \mathbf{v}(\mathbf{k})\mathbf{v}(\mathbf{k})(-\partial f_0/\partial\varepsilon)d\mathbf{k}. \tag{57}$$

Now consider a metal. The volume element in k-space $d\mathbf{k}$ can be replaced by

$$d\mathbf{k} = d\mathbf{S}\frac{d\mathbf{k}}{d\varepsilon}d\varepsilon = \frac{d\mathbf{S}d\varepsilon}{d\varepsilon/d\mathbf{k}} = \frac{d\mathbf{S}d\varepsilon}{|\nabla_{\mathbf{k}}\varepsilon|} \tag{58}$$

where dS is a surface element of the Fermi sphere (see fig. 10) and the gradient is perpendicular to the Fermi surface. With this equation (57) can be written as

$$\underline{\underline{\sigma}} = \frac{e^2}{4\pi^3} \int \frac{\tau \mathbf{v}(\mathbf{k})\mathbf{v}(\mathbf{k})}{|\partial\varepsilon/\partial\mathbf{k}|}(-\partial f_0/\partial\varepsilon)d\mathbf{S}d\varepsilon. \tag{59}$$

The derivative of the Fermi-Dirac distribution function can be approximated by a δ-function which gives

$$\underline{\underline{\sigma}} = \frac{e^2}{4\pi^3\hbar} \int_{FS} \frac{\tau \mathbf{v}(\mathbf{k})\mathbf{v}(\mathbf{k})}{v} d\mathbf{S}. \tag{60}$$

Now the integration is over the Fermi surface. For isotropic or cubic materials the conductivity tensor has only diagonal elements which are all identical. We can then replace $v_x v_x = v_y v_y = v_z v_z = v^2/3$ and get

$$\underline{\underline{\sigma}} = \frac{e^2}{4\pi^3\hbar} \int_{FS} \frac{\tau v}{3} dS. \tag{61}$$

Using for the Fermi Sphere the relations $\int_{FS} k_F dS = 4\pi k_F^3,\ v_F = \hbar k_F/m$ and for the carrier density $n = \frac{1}{4\pi^3}\frac{4\pi}{3}k_F^3$ we get

$$\sigma = \frac{ne^2\tau}{m}. \tag{62}$$

This is precisely the relation that we deduced initially from the Drude model. But note: The physical picture behind it is here completely different. Here only electrons at the Fermi energy are involved. Presumably it is this formal agreement that is responsible for the success of the classical model at all.

So far, we have studied the influence of an external magnetic field on the conductivity or resistivity of a nonmagnetic material. Now we will investigate what happens when the material is ferromagnetic itself.

6 Resistivity of Ferromagnets

Up to now we have studied the galvanomagnetic effects that were generated in nonmagnetic materials by an externally applied magnetic field. When dealing with ferromagnetic materials the sample will show an intrinsic magnetization M which is of course expected to contribute to the Hall effect as well as the magnetoresistance.

The Hall effect, indeed, includes an additional contribution that is directly proportional to the magnetization of the material but it is often much larger than what might be expected when

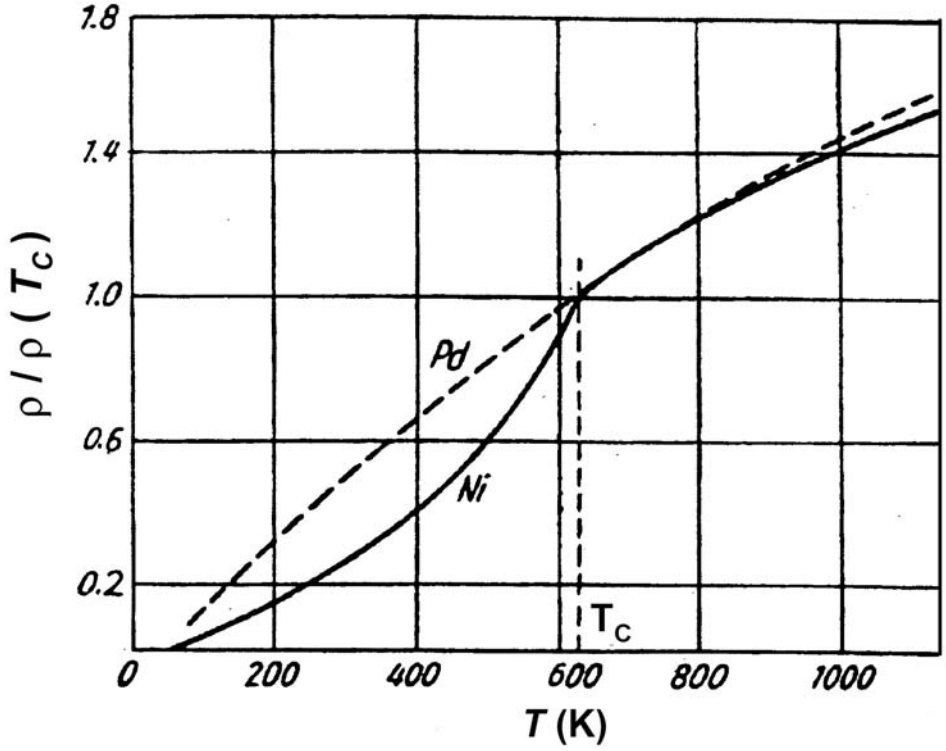

Fig. 11: *Temperature dependence of the relativ resistivities of Ni and Pd normalized to their values at T_c of Ni ($T_c = 631K$)[39].*

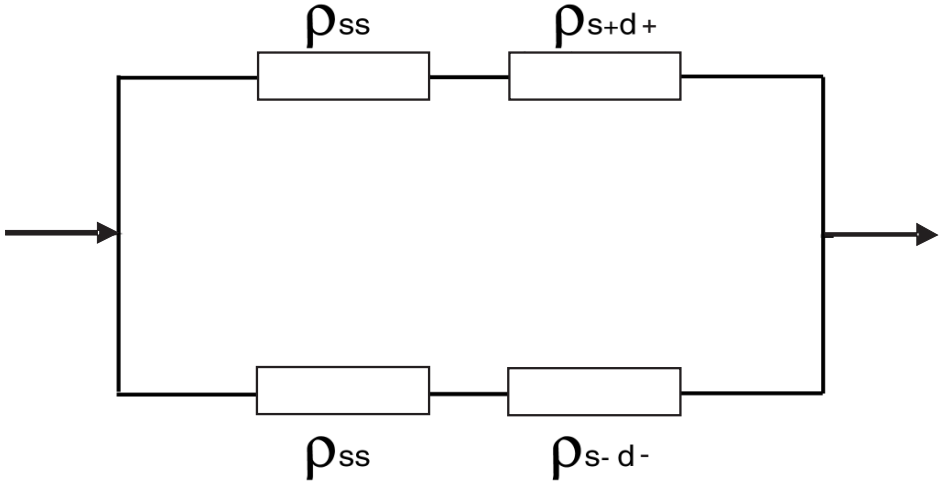

Fig. 12: *Scheme of resistivities due to Mott's two current model. Spin up and spin down channels are signed + and -, respectively.*

$\mu_0 M$ is simply added to the externally applied magnetic field. The effect is therefore called the "anomalous Hall effect". The Hall resistivity may then be written [6]

$$\rho_H = R_0 \mu_0 H + R_s \mu_0 M, \tag{63}$$

where $R_0 \mu_0 H$ is the contribution of the ordinary Hall effect and $R_s \mu_0 M$ is the anomalous

[6] There are different notations used in the literature.

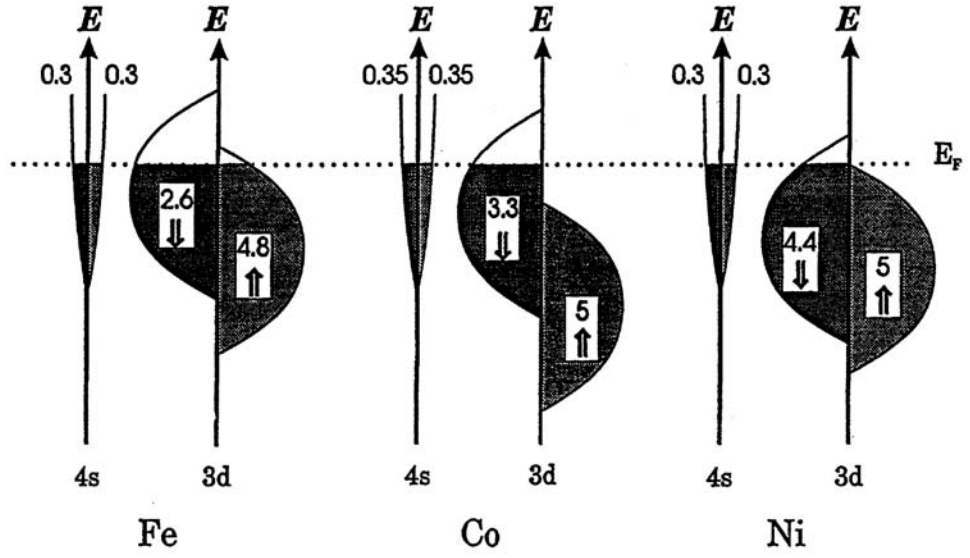

Fig. 13: *Scheme of the densities of states in the sp- and d-bands of ferromagnetic Fe, Co and Ni. The occupation numbers of electrons in the down-spin and up-spin bands are also shown [40, 41].*

contribution. R_S is usually much larger than the ordinary constant R_0. Since M saturates at high magnetic fields the anomalous Hall effect also saturates at high fields. Although the effect has already been discovered more than a century ago by Edwin Hall himself [33], it is still not fully understood. The anomalous Hall effect (AHE) is known to be a consequence of spin-orbit coupling, but the details of the mechanisms that contribute are still subject to controversial discussions.

The anomalous Hall effect has gained new interest because it is also related to the recently discovered Spin-Hall effect. Therefore, two extra contributions are devoted to both these effects in this spring school [34, 35] and therefore we will skip the discussion here.

The other effect caused by the intrinsic magnetization is the anisotropic magnetoresistance (AMR) which was discovered in 1856 by William Thomson the later Lord Kelvin [36]. Before we go into the details of this effect,however, we want to discuss an anomaly that can occur in a ferromagnet without an external magnetic field applied. Fig. 11 shows a comparison of the relativ resistivities of Pd and Ni as a function of temperature [31, 37, 38, 39]. The data are normalized to their values at the Curie temperature of Ni ($631K$). Pd is situated below Ni in the periodic table. Therefore, their electronic structures are quite similar but Pd is paramagnetic at all temperatures while Ni shows the ferromagnetic phasetransition when the temperature decreases below $631K$. Therefore the curves suggest that the differences are due to the formation of a spontaneous magnetization in Ni which is associated with an exchange splitting of the Ni d-states. To explain this behavior Sir N. F. Mott suggested a two current model [42]. It formally splits up the current into two spin channels, one for spin up electrons and the other one for spin down electrons as schematically sketched in Fig. 12. In his approach Mott assumedindependent spin-up and spin-down currents, i.e. the spin information is conserved in the scattering processes. The current is mainly carried by the s-electrons due to their small effective mass (large curvature of the s-bands). The d electrons with their much bigger effective mass (flat d-bands) can contribute only little to the conductivity. The electrons can undergo $s-s$ and $s-d$ scattering transitions where the $s-d$ transitions contribute the most to the resistivity. In

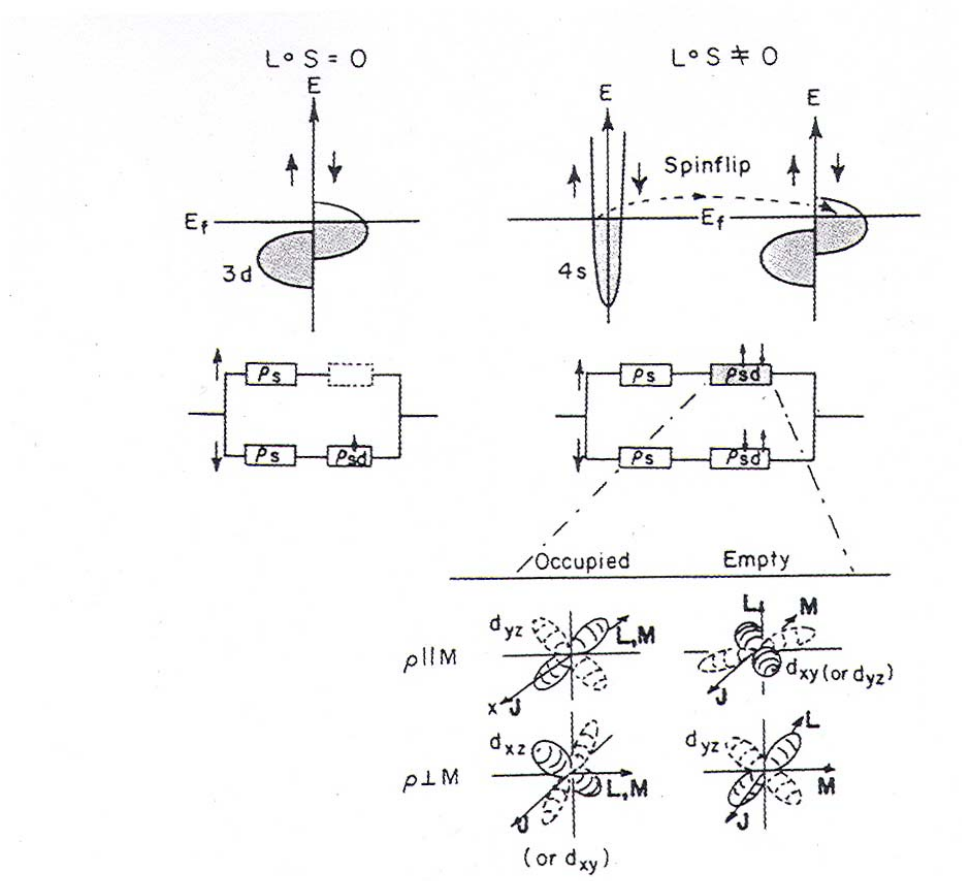

Fig. 14: *(Left: Density of states (3d) of a strong ferromagnet without spin-orbit coupling and the spin-separated resistivity contributions according to Mott's two-current model. In the absence of spin-orbit coupling only $s-d$ scattering processes in the spin-down channel are allowed. Right: Inclusion of spin-orbit coupling opens up the possibility of spin-flip transitions in the $s-d$ channels. As a consequence, also the spin-up channel will now contribute to the conductivity. [52].*

the paramagnetic phase there is no difference in the resistivity of the two spin channels but in the ferromagnetic phase the system develops a spin-dependent asymmetry. Specifically in Ni the majority-spin d-states get completely filled and these states are no longer available for scattering events (Fig. 13) - at least in the absence of spin-orbit coupling. This causes a reduction of the resistivity of the majority spin channel and a reduction of the total resistivity.
A. Fert and I.A. Campbell have later refined Mott's model by allowing also spin-flip scattering due to spin-orbit coupling [43, 44, 45, 46, 47]. The spin-orbit coupling adds a spin-dependent componenet to the scattering potential. In order to understand why spin-orbit coupling may be responsible for spi-flip processes, we have to consider the respective quantum mechanical operator $\mathbf{L} \cdot \mathbf{S}$. It can be written with the aid of ladder operators (raising and lowering operators) in the form

$$\mathbf{L} \cdot \mathbf{S} = L_x S_x + L_y S_y + L_z S_z = L_z S_z + (L^+ S^- + L^- S^+)/2 \tag{64}$$

where $L^\pm = L_x \pm iL_y$ and $S^\pm = S_x \pm iS_y$. Applying $L^\pm$ to a wavefunction has the effect of raising or lowering the m_l quantum number of that wave function

$$L^\pm \psi(m_l) \longrightarrow \psi(m_l \pm 1). \tag{65}$$

Likewise S^+ and S^- can raise or lower the m_s quantum number, i. e. flip a spin. The operator (64) to the wavefunction acts first on the spin and then on the orbital part of the wavefunction and thereby introduces spin-flips between different m_l values, which opens the possibility for additional spin-mixing $s-d$ transitions. In a simple qualitative picture, the spin-orbit coupling enables different transition channels. First of all, s spin-up ($s^\uparrow$) electrons can now scatter into d spin-down hole states ($d^\downarrow$). As a second important mechanism, also transitions of the type $d^\uparrow \rightarrow s^\uparrow$ become possible, which thereby create unoccupied $d^\uparrow$ states. These empty states open up further channels for spin-flip and non spin-flip $s-d$ scattering. However, the scattering probability depends on the $\mathbf{k}$-vector of the electrons and the orbital m_l into which the electron is scattered. This situation is sketched in the bottom, right part of fig. 14, illustrating selected orbitals, which contribute to the resistivity ρ for the two geometries with current flowing parallel and perpendicular to the magnetization M, respectively.
Next we discuss the influence of an external magnetic field on the anisotropic magnetoresistance.

7 Anisotropic Magnetoresistance (AMR)

In ferromagnetic samples the resistance depends on the orientation of the magnetization with respect to the direction of the electric current. Usually the resistivity is larger when the current and the magnetization are parallel and smaller when they are perpendicular. Fig. 15 shows typical examples how the resistivity changes when an external magnetic field is applied [48]. Initially the resistivity increases when an external field is applied parallel to the current and decreases when it is applied perpendicular. These initial effects are due to the reorientation of magnetic domains by the applied field. A field of a few Oersted magnitude is usually sufficient to achieve saturation. Above saturation a slow increase or decrease of both resistivities is observed. The increase can simply be explained by the normal magnetoresistance induced by the Lorentz force, the decrease is attributed to the so called spin disorder resistivity. This contribution becomes particularly importent when the Curie temperature is approached and depends on the scattering of conduction electrons into the exchange split d-states [48]. To obtain values of $\rho_\parallel$ and $\rho_\perp$ which are independent of the externally applied field the measured curves are extrapolated to $\mathbf{B}=0$ as indicated in the figures. The difference between $\rho_\parallel(\mathbf{B}=0)$ and $\rho_\perp(\mathbf{B}=0)$ is called spontaneous resistivity anisotropy. It disappears above T_c because it is associated with the spontaneous internal magnetization. The resistivity anisotropy is often normalized to the average resistivity ρ_0 which is defined as

$$\rho_0 = \rho_{average} = (\frac{1}{3}(\rho_\parallel(B=0) + \frac{2}{3}\rho_\perp(B=0)), \tag{66}$$

where $\rho_\parallel(B=0)$ and $\rho_\perp(B=0))$ are the extrapolated values. This ratio is called the anisotropic magnetoresistivity ratio or coefficient. Note, that the average resistivity defined above is not in general identical with the resistivity of the field free demagnetized sample [52]. The anisotropic magnetoresistance is caused by anisotropic scattering of the charge carriers by spin-orbit coupling. The resistance varies with the orientation of the d-orbitals parallel or perpendicular to the magnetic field.
Now consider a thin homogeneous strip of a magnetoresistive material, e. g. permalloy, with a large aspect ratio, i.e. its length is much larger than its width. If the sample thickness exceeds a certain value (a few $10\ nm$) we can expect the magnetization to lie in the plane of the film.

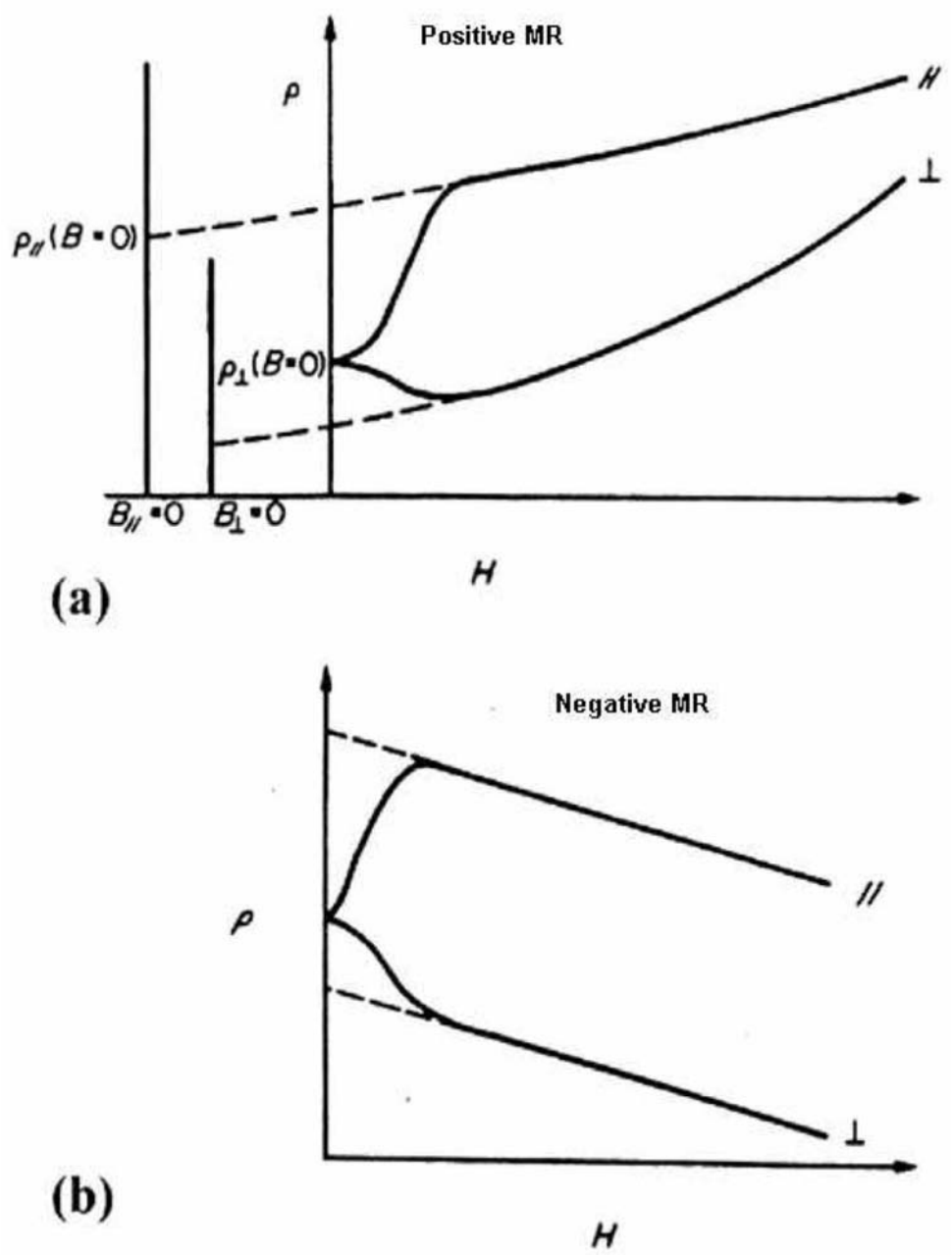

Fig. 15: *schematic resistivity change for ferromagnets. The extrapolated resistivities are also shown. After saturation of the magnetization the resistivity either increases (a): normal positive magnetoresistance or (b) decreases due to the reduction of spin-disorder. [48].*

To minimize the stray field the magnetization will orient parallel to the long axis of the film which therefore is the easy axis.[7] We identify this axis with the z'-axis of an orthonormalized coordinate sytem and the perpendicular in plane direction with the x'-axis.[8] In this case we can

[7] The easy axis of a sample is the axis along which the sample is most readily magnetized.

[8] In the following we will use two coordinate systems: one (x', y', z') in which the magnetization is fixed with the z' axis. The other one $(x, y = y', z)$ which is fixed to the sample geometry can be rotated about the common y-axis by an arbitrary angle φ (see Figs. 16 and 17).

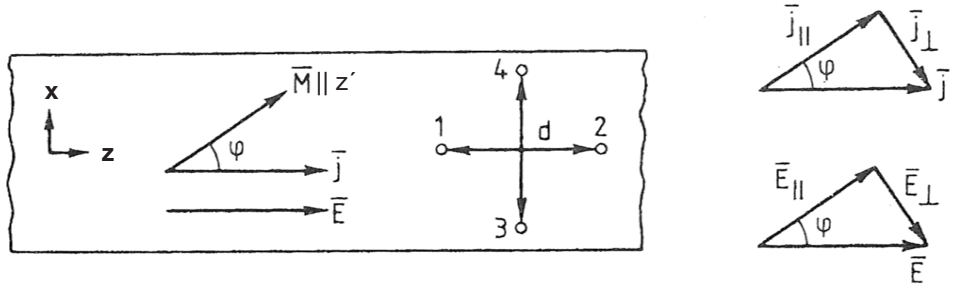

Fig. 16: *Geometric arrangement for the calculation of anisotropic magnetoresistance and planar Hall effect components as described in the text [54, 49].*

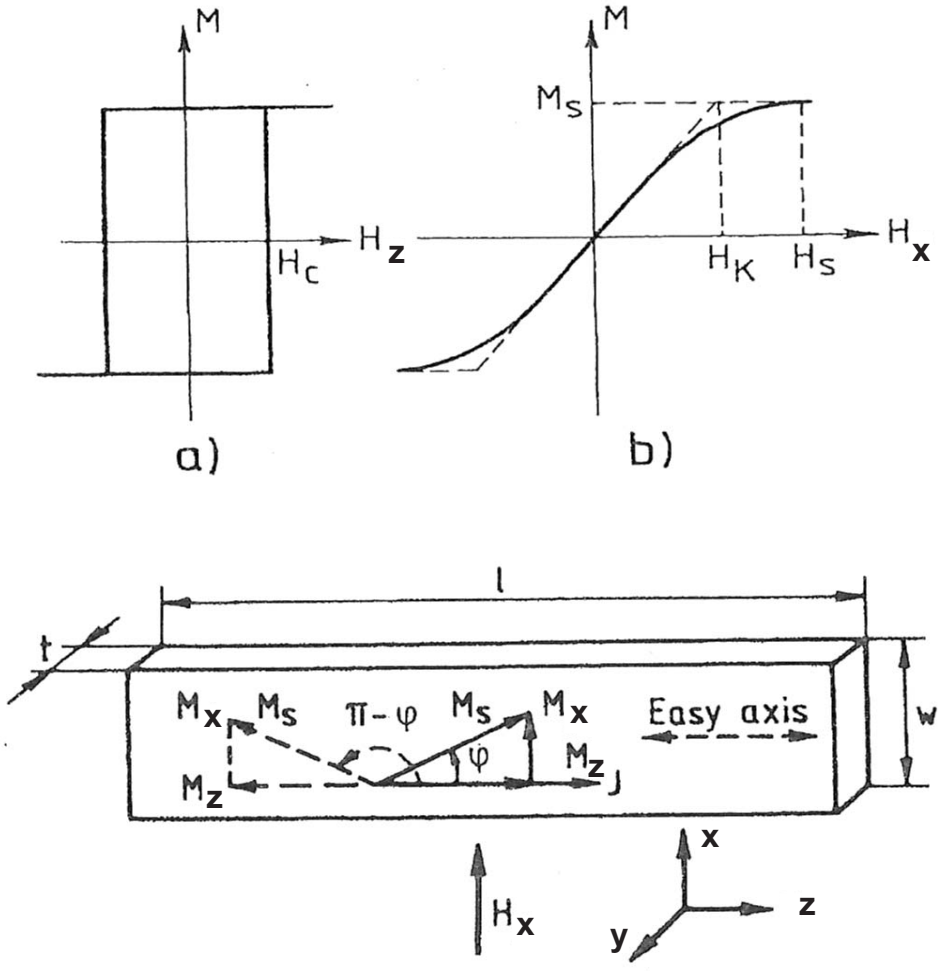

Fig. 17: *Idealized easy axis (a) and hard axis (b) magnetization curves of an in plane magnetized anisotropic magnetic thin film as shown in the lower figure. The z-axis (long axis) is the easy axis and the x-axis the hard axis. The rotation of the magnetization upon application of an external magnetic field parallel to the hard axis is indicated. [54, 49].*

easily guess the relation between an applied electric field and the current density achieved. It is:

$$\begin{pmatrix} E_{x'} \\ E_{y'} \\ E_{z'} \end{pmatrix} = \begin{pmatrix} \rho_\perp & -\rho_H & 0 \\ \rho_H & \rho_\perp & 0 \\ 0 & 0 & \rho_\parallel \end{pmatrix} \begin{pmatrix} j_{x'} \\ j_{y'} \\ j_{z'} \end{pmatrix} \quad \text{or} \quad \mathbf{E}' = (\rho_{i'j'}(\mathbf{M}))\mathbf{j}' \tag{67}$$

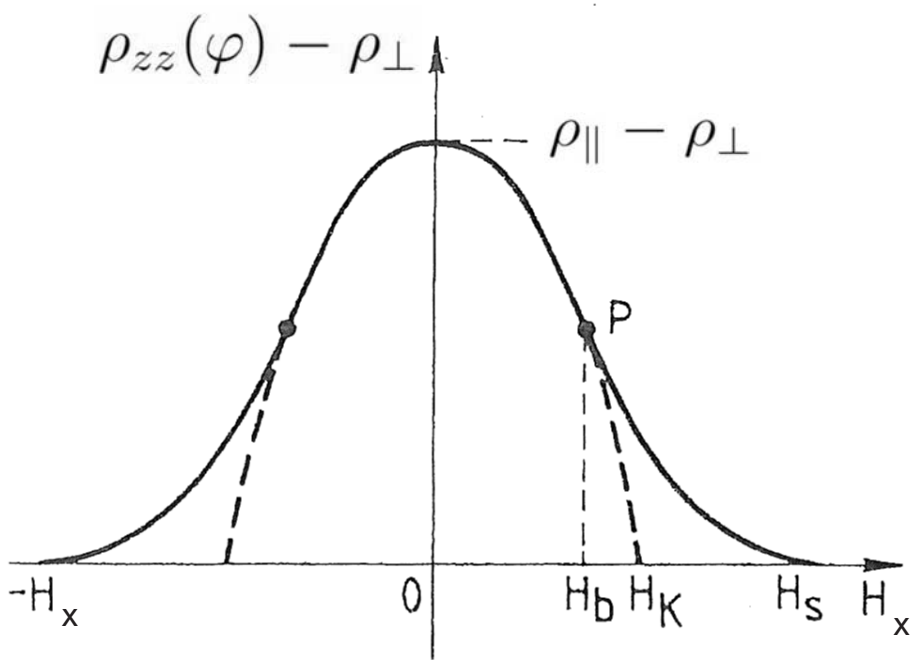

Fig. 18: *Response of a permalloy thin-film magnetoresistor as described in the text [54, 49].*

where $\rho_\parallel$ and $\rho_\perp$ are obviously in accordance with the description given above. ρ_H is the resistivity corresponding to the anomalous Hall effect which we will not further consider. However, in this form the resistivity tensor is only valid when the magnetization of the sample is fixed to the easy axis. For a detailed analysis of the AMR we need a more general form of the tensor where the current density $\mathbf{j}'$ and the magnetization $\mathbf{M}$ include an arbitrary angle φ in the (x', z')-plane. We derive this form by a similarity transformation of the AMR-matrix in the following way:
We assume that the coordinate system defined above is fixed with the magnetization: $M \parallel z'$. We rotate the sample and with it $\mathbf{E}'$ and $\mathbf{j}'$ by an angle φ and define a new rotated coordinate system (x, y) so that the new orientation of the long sample axis is parallel to the new z-axis together with the applied field $\mathbf{E}$ and the current density $\mathbf{j}$. This situation is indicated in Fig. 16. For the equation (67) to remain valid we have to rotate $\mathbf{E}$ and $\mathbf{j}$ back to the old system:

$$\mathbf{E}' = R(\varphi)\mathbf{E} \quad \text{and} \quad \mathbf{j}' = R(\varphi)\mathbf{j} \tag{68}$$

where $R(\varphi)$ is the transformation matrix that provides the backrotation. Thus from equation (67) we get

$$\mathbf{E}' = R(\varphi)\mathbf{E} = (\rho_{i'j'}(\mathbf{M}))R(\varphi)\mathbf{j} = (\rho_{i'j'}(\mathbf{M}))\mathbf{j}'. \tag{69}$$

where $(\rho_{i'j'}(\mathbf{M}))$ is the resistivity tensor defined above. Using the associativity of matrix multiplication we therefore get the AMR-matrix in the transformed coordinates:

$$\rho_{ij}(\mathbf{M}) = R^{-1}(\varphi)(\rho_{i'j'}(\mathbf{M}))R(\varphi)$$

$$= \begin{pmatrix} cos\varphi & 0 & sin\varphi \\ 0 & 1 & 0 \\ -sin\varphi & 0 & cos\varphi \end{pmatrix} \begin{pmatrix} \rho_\perp & -\rho_H & 0 \\ \rho_H & \rho_\perp & 0 \\ 0 & 0 & \rho_\parallel \end{pmatrix} \begin{pmatrix} cos\varphi & 0 & -sin\varphi \\ 0 & 1 & 0 \\ sin\varphi & 0 & cos\varphi \end{pmatrix}$$

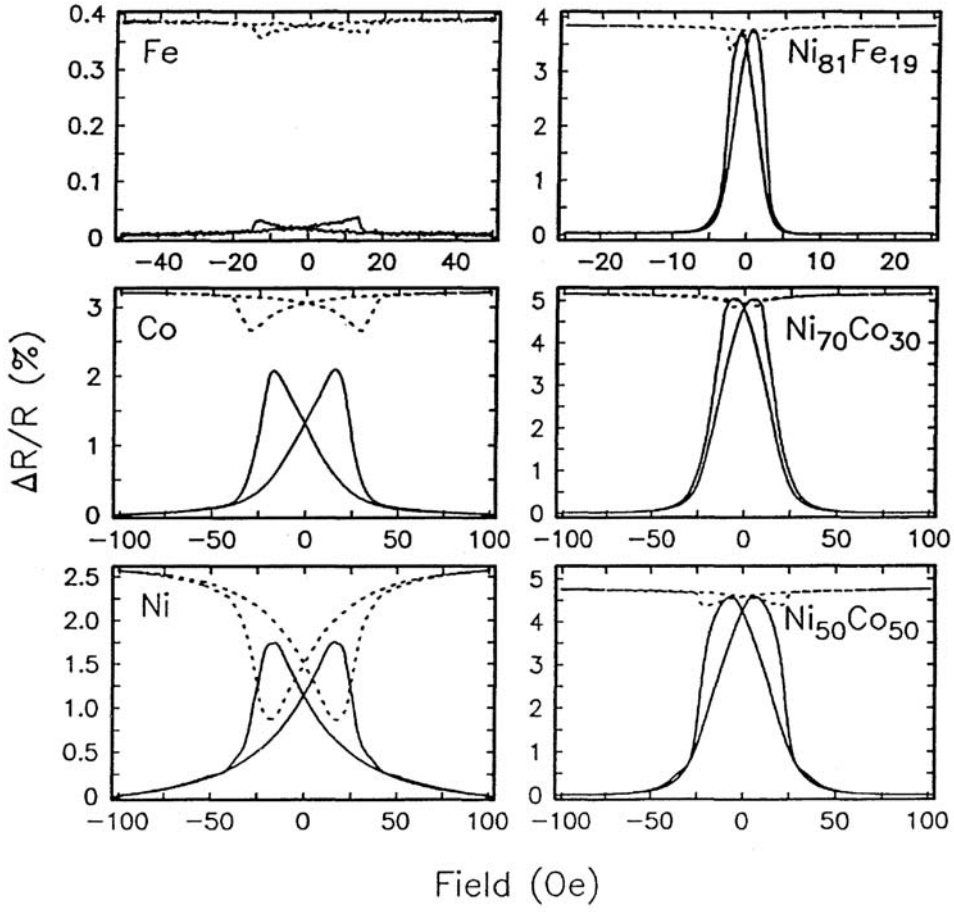

Fig. 19: *Examples of the anisotropic magnetoresistance effect in sputtered polycrystalline films of Fe, Co, Ni and $Ni_{81}Fe_{19}$ (permalloy), $Ni_{70}Co_{30}$ and $Ni_{50}Co_{50}$. The full and dotted lines correspond to magnetic field applied orthogonal and parallel to the current respectively in the plane of the films. The films in each case are ≈ 1000 Å thick [40].*

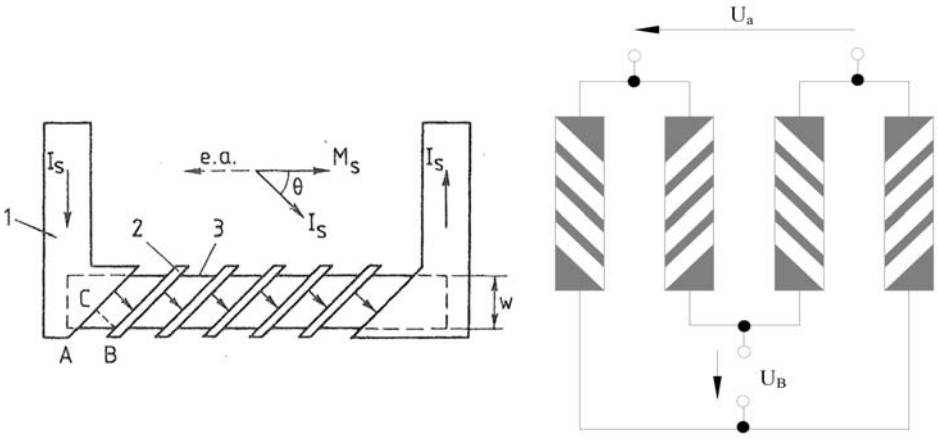

Fig. 20: *left: Scheme of a permalloy (3) barber-pole magnetoresistor with canted conductor strips(2). Magnetization and current direction is indicated. right: Schematic Wheatstone-bridge arrangement of four barber poles. [49].*

$$= \begin{pmatrix} \rho_\perp cos^2\varphi + \rho_\parallel sin^2\varphi & -\rho_H cos\varphi & -\rho_\perp sin\varphi cos\varphi + \rho_\parallel cos\varphi sin\varphi \\ \rho_H cos\varphi & \rho_\perp & -\rho_H sin\varphi \\ -\rho_\perp sin\varphi cos\varphi + \rho_\parallel cos\varphi sin\varphi & \rho_H sin\varphi & \rho_\perp sin^2\varphi + \rho_\parallel cos^2\varphi \end{pmatrix} \quad (70)$$

Thus for the electric field applied in the z-direction we have

$$E_z = \rho_{zz}(\varphi) j_z \quad (71)$$

where

$$\rho_{zz}(\varphi) = \rho_\perp sin^2\varphi + \rho_\parallel cos^2\varphi = \rho_\perp + (\rho_\parallel - \rho_\perp) cos^2\varphi. \quad (72)$$

This is often rewritten as

$$\rho_{zz}(\varphi) = (\frac{1}{3}\rho_\parallel + \frac{2}{3}\rho_\perp) + (\rho_\parallel - \rho_\perp)(cos^2\varphi - \frac{1}{3}) \quad (73)$$

where $\rho_0 = (\frac{1}{3}\rho_\parallel + \frac{2}{3}\rho_\perp)$ is the average resistivity defined above. The resistivity coefficient is then defined as

$$\frac{\rho_{zz}(\varphi) - \rho_0}{\rho_0} = \frac{\Delta\rho}{\rho_0} = \frac{(\rho_\parallel - \rho_\perp)}{(\frac{1}{3}\rho_\parallel + \frac{2}{3}\rho_\perp)}(cos^2\varphi - \frac{1}{3}). \quad (74)$$

By applying an electric field in the z direction we not only create a current j_z in the direction of the applied field but also generate an electric field perpendicular to this current.

$$E_x = \rho_{xz}(\varphi) j_z \quad (75)$$

where

$$\rho_{xz}(\varphi) = (\rho_\parallel - \rho_\perp) cos\varphi sin\varphi = (\rho_\parallel - \rho_\perp)\frac{1}{2} sin2\varphi \quad (76)$$

This effect is called the "planar Hall effect" or "pseudo Hall effect" and is believed to have some potential for applications with micro- or nanostructured spintronic devices [50, 51]. It is zero when the magnetization is parallel or perpendicular to the easy axis.

In the following we will calculate the AMR response of a sample under somewhat idealized conditions. For instance we will ignore any demagnetizing effects and assume idealized hysteresis conditions. In accordance with our above premisis we consider a ferromagnetic thin film (e.g. permalloy) with a large aspect ratio. We also assume that the magnetization is in the film plane. Without a magnetic field applied the magnetization direction is parallel to the easy axis of the film which again we identify with the long z-axis of our specimen. If a magnetic field is varied parallel to this easy axis one observes a rectangular hysteresis (Fig. 17) [49]. On the contrary, if the external magnetic field is varied along the coplanar hard axis the magnetization in this direction will show a linear slope and finally saturate. The Magnetic moment of the film rotates towards the hard axis. During this procedure the film is divided into elongated antiparallel domains, whose magnetizations rotate at an angle φ for the parallel ones and $\pi - \varphi$ for the antiparallel ones when the vertical field H_x is applied in the film plane [49] (Fig. 17). Neglecting demagnetization effects we have the relation:

$$\frac{M_x}{M_s} = sin\varphi = \frac{H_x}{H_K} \quad \text{for} \quad -H_K \leq H_x \leq H_K. \quad (77)$$

Here M_x is the x-component of the magnetization, M_s is the saturation magnetization H_x is the applied magnetic field and H_k is the magnetization where saturation sets in. Introducing this result into equation (72) gives:

$$\rho_{zz}(\varphi) = \rho_\perp + (\rho_\parallel - \rho_\perp)(1 - (\frac{H_x}{H_K})^2). \quad (78)$$

The graph of this equation is an upside down parabola with the maximum at $H_x = 0$ and it ends on the abscissa where the H_x value reaches the saturation point H_K. This graph is plotted in Fig. 18. Experimentally it is found that the function more smoothly approaches the abscissa (solid line in the figure). This discrepancy is attributed to the demagnetizing fields that we have ignored so far. As a consequence saturation is not reached at H_K but at $H_s = H_K + H_d$ where H_d is the demagnetizing field. It is clear from the curve that in the vicinity of zero field ($H_x = 0$) the magnetoresistor is of low sensitivity and due to its quadratic response also highly nonlinear. Moreover it cannot detect the polarity of the applied external field. For sensor applications it is therefore desirable to shift the operating point to the inflection point of the curve (Fig. 18) where the highest sensitivity can be achieved and the response is approximately linearized. At this point the orientation of the field can also be detected. The shift of the operation point can either be achieved by a biasing field of a nearby permanent magnet (just as in the case of the Lorentz magnetoresistance described above) or by use of a so called barber-pole structure to be discussed below. The sensitivity is optimal when the angle between the magnetization and the current direction is kept at about 45^o. This principle has been used in AMR-read heads which have been used for a few years in hard disk technology before they were replaced by the GMR based spin-valve read heads. Details on AMR-read head technology are found in the literature [52, 53, 54, 55]. Fig. 19 shows magnetoresistance runs for thin films of Fe, Co, Ni, permalloy $Ni_{81}Fe_{19}$, and two nickel-cobalt alloys [40]. Except for Fe and Ni the sensitivity is larger when the magnetization is perpendicular to the current (solid lines) rather than parallel (dotted lines). The effect is in the range of a few percent. The curves show a clear hysteresis. Obviously the samples do not follow our idealized magnetization curve and show a little coercivity which corresponds to the position of the two maxima. The magnetization cannot follow the external field immediately. The occurance of the hysteresis is attributed to an easy axis dispersion in the literature [49]. This means that the sample easy axis is a macroscopic average, but locally inside the sample the easy axes might show in slightly different directions in different domains. During the magnetization procedure the sample splits up into a multidomain structure with longitudinal domains parallel to the average easy axis. The switching behavior of these domains is responsible for the hysteresis. It was also reported that a slight vertical remanence could be observed when the vertical field was reduced to zero.

As pointed out above the optimum operating point of an AMR-sensor is obtained when the current and the magnetization include an angle of about 45^o. There exists an alternative technique to applying a bias field, namely to force the current into an angle of 45^o with respect to the magnetic easy axis. This is done in a barber-pole structure (Fig. 20). The name stems from the similarity of the structure with barber poles which since the middle ages have been used as signatures of barber shops and are sometimes still used today. The barber pole sensor consists of a permalloy magnetoresistive film with its easy axis parallel to its length. It is covered by conductor strips which are canted at 45^o. The strips are up to 50 times better conductors than the magnetoresistive layer. This forces the equipotential lines inside the magnetoresistor parallel to the strips so that the current flow in the magnetoresistor is perpendicular to the strips, i. e. at 45^o with respect to the magnetization. Miniaturized commercial sensors combine four such barberpoles in a Wheatstone bridge arrangement. A typical chip size is $1.6mm \times 1.6mm$ at resistance of $1.7K\Omega$. They are used in contactless angular or linear position measurements. They are characterized by high sensitivity and stability and high reliability. AMR-sensors are very sensitiv and operate in the $\approx 1nT$ to $1mT$ range in contrast to Hall sensors which operate in the $\approx 0.1mT$ to $100T$ range [56, 57].

8 Conclusion

In this contribution we have discussed galvanomagnetic transport in nonmagnetic and ferromagnetic materials. All the effects are bulk effects and since they are at the very basis of spintronics, it is necessary to consider them in many spintronic measurements and devices. Due to their high reliability the effects have been and are still partially used in technology, but are also slowly replaced by other spintransport effects, such as giant or tunneling magnetoresistance. We have also shown that quantum mechanical techniques are necessary to properly interpret the eletrical transport phenomena. From the theoretical point of view particularly the influence of spin-orbit coupling needs further detailed analysis. For reasons of clarity, we have taken a somewhat simplified point of view in our discussion of the effects, e.g. considering only the influence of a single or at most two bands. In reality even more bands need to be taken into account. Moreover, there are additional effects, which become important in confined geometries like domain wall resistivity or domain wall pinning, which can superimpose the described behavior and are dealt with in other contributions of this Spring School.

Appendix

A Derivation of Equation (32)

In the following calculation we neglect the fact that the conductivity and with it the currents and velocities in the (x,y)-plane are reduced by factors $1/(1+(\mu_{e,h}B_z)^2) = 1/(1+(\tau_{e,h}\omega_c^{(e,h)})^2)$, respectively [9], because these factors approximately cancel during the calculation and for weak magnetic fields are close to 1, anyway: $(\tau\omega_c \ll 1)$.
Then to calculate the Hall field E_H we start with the Lorentz force:

$$F_L = q(\mathbf{v}\times\mathbf{B}) = q\begin{pmatrix} v_yB_z - v_zB_y \\ v_zB_x - v_xB_z \\ v_xB_y - v_yB_x \end{pmatrix}. \tag{79}$$

Since at stationary conditions we will have current flowing only in the x direction, i.e. $\mathbf{v} = (v_x, 0, 0)$, and as $\mathbf{B} = (0, 0, B_z)$ the active component of the Lorentz force is

$$F_{L,y} = -qv_xB_z, \tag{80}$$

where for electrons $q = -e$ and $v_x = -|v_x| = v_x^{(e)} < 0$ and for holes $q = +e$ and $v_x = v_x^{(h)} > 0$. Thus, the resulting Lorentz force is

$$F_{L,y}^{(e)} = -(-e)(v_x^{(e)}B_z) = ev_x^{(e)}B_z \quad \text{for electrons} \tag{81}$$

and

$$F_{L,y}^{(h)} = -(e)(v_x^{(h)}B_z) = -ev_x^{(h)}B_z \quad \text{for holes.} \tag{82}$$

Neglecting the quadratic terms in equations (25) and (26) and by comparison with equation (13) we write $v_x^{(e)} = -\mu_eE_x$ and $v_x^{(h)} = \mu_hE_x$. Including the action of the Hall field E_H we get:

$$F_y^{(e)} = -e(E_H - v_x^{(e)}B_z) = -e(E_H + \mu_eE_xB_z) \quad \text{for the electrons} \tag{83}$$

[9] compare with equations (25) and (26)

and

$$F_y^{(h)} = e(E_H - v_x^{(h)} B_z) = e(E_H - \mu_h E_x B_z) \quad \text{for the holes.} \tag{84}$$

Putting these forces into the respective equations of motion gives

$$m_e \frac{dv_y^{(e)}}{dt} + \frac{m_e}{\tau_e} v_y^{(e)} = -e(E_H + \mu_e E_x B_z) \quad \text{for the electrons} \tag{85}$$

and

$$m_h \frac{dv_y^{(h)}}{dt} + \frac{m_h}{\tau_h} v_y^{(h)} = e(E_H - \mu_h E_x B_z) \quad \text{for the holes.} \tag{86}$$

At steady state the time derivatives are zero and therefore the currents in the y-direction for the electrons and for the holes are given by

$$j_y^{(e)} = -e n_e v_y^{(e)} = e n_e \mu_e (E_H + \mu_e E_x B_z) \tag{87}$$

and

$$j_y^{(h)} = e n_h v_y^{(h)} = e n_h \mu_h (E_H - \mu_h E_x B_z). \tag{88}$$

Once equilibrium is reached, there will be no net current in the y-direction:

$$j_y^{(e)} + j_y^{(h)} = 0. \tag{89}$$

Here it is ***not*** required that the force generated by the Hall field E_H cancels the Lorentz forces for the electrons and holes separately. However the currents in the y-direction cancel each other. The total current in the y-direction then gets

$$j_y^{(e)} + j_y^{(h)} = 0 = e n_e \mu_e (E_H + \mu_e E_x B_z) + e n_h \mu_h (E_H - \mu_h E_x B_z) \tag{90}$$

and thus

$$(n_e \mu_e + n_h \mu_h) E_H = (n_h \mu_h^2 - n_e \mu_e^2) E_x B_z. \tag{91}$$

Finally, replacing $E_x = j_x / \sigma_{ambipolar} = j_x / [e(n_e \mu_e + n_h \mu_h)]$ we derive the Hall voltage:

$$U_H = E_H \cdot b = \frac{n_h \mu_h^2 - n_e \mu_e^2}{e(n_h \mu_h + n_e \mu_e)^2} j_x B_z \cdot b = \frac{n_h - n_e(\mu_e/\mu_h)^2}{e(n_h + n_e \mu_e/\mu_h)^2} \, iB/d \tag{92}$$

where the ratio of the mobilities has been introduced.

References

[1] N. W. Ashcroft and N. D. Mermin, Solid State Physics (Saunders College, 1976).

[2] J. F. Nye, Physical Properties of Crystals, At The Clarendon Press, Oxford (1972)

[3] L. Onsager, Phys. Rev. **37**, 405 (1931); ibid. **38**,2265(1931)

[4] P. Drude,Annalen der Physik **1**, 566 (1900); ibid **3**, 369 (1900)

[5] E.H. Hall: "On a New Action of the Magnet on Electric Currents". Am. J. Math. **2**, p.287-292 (1879)

[6] C. M. Hurd, The Hall Effect in Metals and Alloys, Plenum Press, New York (1972)

[7] C. L. Chien, C.R. Westgate, The Hall Effect and its Applications, Plenum Press, New York (1980)

[8] H. Ibach, H. Lüth, Solid State Physics, Springer, Berlin,Heidelberg, New York (2003)

[9] O. Madelung, Grundlagen der Halbleiterphysik, Springer Verlag, Berlin, Heidelberg, New York (1970)

[10] H. Weiss und H. Welker, Zur transversalen magnetischen Widerstandsänderung von InSb, Z. Phys. **138**, 322 (1954).

[11] F. J. Blatt, Physics of Electronic Conduction in Solids, Mc Graw Hill, New York (1968)

[12] J. M. Ziman, Electrons in Metals, A short guide to the Fermi surface,Contemp. Phys. **3**, 241; ibid. 321; ibid. 401; ibid. **4**, 1; ibid. 81 (1962); J. M. Ziman, Principles of the Theory of Solids, Cambridge, At the University Press (1969)

[13] O. Madelung und H. Weiss, Die elektrischen Eigenschaften von Indiumantimonid II, Z. Naturforschg. **9a**, 527 (1954)

[14] H.Weiss, Structure and Application of Galvanomagnetic Devices, Pergamon Press, Oxford (1969)

[15] K. Seeger, Semiconductor Physics, 5th edition, Springer Verlag, Berlin, Heidelberg (1991)

[16] P.Y. Yu, M.Cardona, Fundamentals of Semiconductors, 3rd Edition, Springer Verlag, Berlin, Heidelberg, New York (2001)

[17] L. J. van der Pauw: A method of measuring specific resistivity and Hall effect of discs of arbitrary shape. Philips Research Reports **13**, (1) 1 (1958); L.J. van der Pauw, A method of measuring the resistivity and Hall coefficient on lamellae of arbitrary shape. Philips Technical Review **20**, 220 (1958); http://www.ecse.rpi.edu/ schubert/More-reprints/

[18] O.M. Corbino, Elektromagnetische Effekte, die von der Verzerrung herrühren, welche ein Feld an der Bahn der Ionen in Metallen hervorbringt, Phys. Z. **12**, 561 (1911)

[19] M. Kohler, Annalen der Physik **424**, 211 (1938); ibid **441**, 18 (1950) and references therein.

[20] J.-P. Jan, Galvanomagnetic and Thermomagnetic Effects in Metals, in: F. Seitz, D. Turnbull (Edts) Solid State Phys. Vol. **5**, p. 1, Academic Press, New York (1975)

[21] P.L. Rossiter, Metals and Alloys, Conductivity in, Encyclopedia of Applied Physics, Vol. **10**, p.163, VCH Publishers (1994)

[22] P. K. Siwach, H. K. Singh, and O. N. Srivastava, J. Phys.: Condens. Matter **20**, 273201 (2008)

[23] G. Bublitz, Messung magnetischer Gleichfelder mit Wismutspiralen und Wismutplatten, ATM **5**, 391 (1937)

[24] H. Weiss, The "Feldplatte" a new semiconductor magnetoresistance device, IEEE Transactions on Magnetics **2**, 540 (1966)

[25] H. Weiß, Galvanomagnetische Bauelemente, Festkörper Probleme **7**, 200-216, Springer Verlag, Berlin, Heidelberg (1967); H. Welker, Chemie-Ing.-Techn. **37**, 916 (1965)

[26] Fig. taken from: K. Mertens, http://www.et.fh-muenster.de/persons/mertens/se_folien/sekap4.pdf

[27] S.A. Solin and L.R. Ram-Mohan, Geometry Driven Magnetoresistance, p. 2979 in: H. Kronmüeller, S. Parkin (Eds.), Handbook of Magnetism and Advanced Magnetic Materials, Vol. **5**: Spintronics and Magnetoelectronics, John Wiley & Sons (2007); S. A. Solin, T. Thio, D. R. Hines and J. J. Heremans, Science **289**, 1530 (2000); S. A. Solin, D. R. Hines and A. C. H. Rowe, Appl. Phys. Lett. **80**, 4012 (2002).

[28] M. Holz, O. Kronenwerth, D. Grundler, Magnetoresistance of semiconductor-metal-hybrid structures: The effect of material parameters and contact resistance. Phys. Rev. **B 67**, 195312 (2003); Appl. Phys. Lett. **86**, 072513 (2005); Appl. Phys. Lett. **87**, 172501 (2005); M. Hoener, O. Kronenwerth, Ch. Heyn, D. Grundler, and M. Holz, J. Appl. Phys. **99**, 036102 (2006); C. H. Möller, O. Kronenwerth, Ch. Heyn, and D. Grundler, Appl. Phys. Lett. **84**, 3343 (2004); Fig.: by M. Holz In: Matthias Hoener, Optimierung von Extraordinary-Magnetoresistance-Magnetfeldsensoren aus mikrostrukturierten Metall-Halbleiter-Hybridstrukturen, Diplomarbeit, Universität Hamburg (2004); www.physik.tu-berlin.de/cluster/Dipl.20062004.pdf

[29] Chuan-Bing Rong, Hong-Wei Zhang, Ji-Rong Sun, and Bao-Gen Shen, Enhanced extraordinary magnetoresistance in the semiconductor-metal hybrid structure with three current leads, Appl. Phys. Lett. **89**, 052503 (2006)

[30] O. Madelung, Introduction to Solid State Theory, Springer Verlag, Berlin, Heidelberg, New York (1978) [The original German Version appeared in three volumes: O. Madelung, Festkoerpertheorie I-III, Springer Verlag Berlin, Heidelberg, New York (1972)];

[31] J. M. Ziman, Electrons and Phonons, Clarendon Press, Oxford (2001)

[32] see ref. 1 Chapter 2

[33] E. H. Hall, Philos. Mag. **10**, 301 (1880); **12**, 157 (1881)

[34] Y. Mokrousov, this springschool

[35] A. Fert, this springschool

[36] W. Thomson, On the electrodynamic qualities of metals - effects of magnetization on the electric conductivity of nickel and of iron, Proc. Royal Soc. London **8**, 546-555 (1857)

[37] J. G. G. Conybeare, Proc. Phys. Soc. **49**, 29 (1937)

[38] H. H. Potter, Proc. Phys. Soc. **49**, 671 (1937)

[39] R. Gross, A. Marx, Spintronics; http://www.wmi.badw.de/teaching/Lecturenotes/

[40] S.S.P. Parkin, 2.4 Giant Magnetoresistance and Oscillatory Interlayer Coupling in Polycrystalline Transition Metal Multilayers, in: B. Heinrich and J.A.C. Bland (Eds.) Ultrathin Magnetic Structures II, Springer-Verlag Berlin Heidelberg 1994

[41] J. Mathon: Contemp. Phys. **32**, 143 (1991)

[42] N. F. Mott, Proc. Roy. Soc. **153**, 699(1936) and Adv. Phys. **13**, 325(1964)

[43] I. A. Campbell, A. Fert, A. R. Pomeroy, Phil. Mag **15**, 977 (1967)

[44] A. Fert, I. A. Campbell, Phys. Rev. Lett. **21**, 1190 (1968)

[45] I. A. Campbell, A. Fert, O.Jaoul, J. Phys. C, Metal Phys. Suppl. **1**, S95 (1970)

[46] A. Fert, I. A. Campbell, J.Phys. F., Metal Phys. **6**, 849 (1976)

[47] I. A. Campbell, A. Fert, in Ferromagnetic Materials, Wohlfarth (Ed.), Vol **3**, chapter 9, p.747, North Holland Publ. Comp., Amsterdam (1982)

[48] A. Fert, C. Vouille, 30. IFF-Ferienkurs, Magnetische Schichtsysteme, Forschungszentrum Jülich 1999

[49] P. Ciureanu, Magnetoresistive Sensors, Chapter 5 in: P. Ciureanu and S. Middelhoek (Edts.), Thin Film Resistive Sensors, IOP Publishing (1992)

[50] L. Ejsing, M. F. Hansen, A. K. Menon, H. A. Ferreira, D. L. Graham, and P. P. Freitas, Appl. Phys. Lett. **84**, 4729 (2004)

[51] Y. S. Huang, C. C. Wang, A. O. Adeyeye, and D. Tripathy, J. Appl. Phys. **99**, 08C508 (2006)

[52] R. C. O'Handley, Modern Magnetic Materials, Principles and Applications, John Wiley & Sons, New York (2000)

[53] R. P. Hunt, IEEE Trans. MAG-**7**, 150 (1971)

[54] D. A. Thompson, L. T. Romankiw, and A. F. Mayadas, IEEE Trans. MAG-**11**, 1039 (1975)

[55] T. R. McGuire, R. L Potter: IEEE Trans. Mag. MAG-11, 1018 (1975)

[56] R. Steiner Vanha, H. Baltes, Lateral and Vertical Hall Microsystems,in: H. Baltes, W.Göpel, J.Hesse (Eds.), Sensors, Vol. **8** Update, Wiley-VCH Verlag, Weinheim (2001)

[57] Slawomir Tumanski, Thin Film Magnetoresistive Sensors, IOP Publishing, Bristol (2001)